國立臺灣大學生命科學院動物學研究所

碩士論文

Institute of Zoology

College of Life Science

National Taiwan University

Master Thesis

異位表現 *Odysseus* 造成有絲分裂的缺陷

Ectopic expression of *Odysseus* causes mitotic defects

林姵君

Pei-Chun Lin

指導教授：丁照棣

Advisor : Chau-Ti Ting

中華民國98年7月

July, 2009

Acknowledgements

在台大動物所歷經兩年的學習後，我有所成長，也深懷感激。

首先，很感謝我的指導教授丁照棣老師，願意讓我在碩一上學期快要結束的時候進入實驗室，帶領我很快的熟悉果蠅實驗的操作，以及許多背景知識的建立。這一年多的時間裡，我學習到很多，很多老師教我的，和讓我領悟到的。在實驗的過程中，東海大學的蔡玉真老師教我如何進行果蠅眼睛的免疫染色，並且非常熱心的提供許多建議，陽明大學的廖國楨老師教我辨識胚胎齡期和觀察，以及國衛院的陳俊宏老師，在實驗設計上的指導，老師們的協助，讓我有今天的成果，很感謝。也謝謝張慧羽老師，方淑老師，王弘毅老師，和曹順成老師，閱讀，修改這本論文，並且在想法上，有許多指點，讓我的論文能做更好的呈現。

謝謝這段日子，實驗室裡陪伴著我的每個成員。最最感謝的是雅仁學姐，在實驗和想法上，都教會我許多，並且分擔著我的壓力，不斷地鼓勵我。謝謝小春，願意花時間聽我報告，給予建議，還在出國前送了我一套漂亮的新衣服。謝謝文喬，雖然自己的事情很忙碌，還是很關心我，並且不時帶來歡笑。謝謝景賀，一起留在實驗室的很多個晚上，幫我買晚餐，陪我做實驗和講話讓我不無聊，也幫了我許多忙，祝你早日交到很棒的女朋友！謝謝Kevin幫忙修改我的論文文法，還曾經為了幫我準備上台報告，弄到半夜四點，真是辛苦你了！還有坐在隔壁的小菊，總是和我分享無止盡的話題跟生活經驗，增添了許多歡樂時光，謝謝你。謝謝心彥，帶來各式各樣好吃的食物以及甜點食譜，每一樣都很美味喔！謝謝統計很厲害，喜孜孜的胖丁；唱歌key超高資訊豐富的士又；講話常常有聽沒有懂的名師董強；我的第一個法國朋友，松鼠寶寶的奶爸Stephane，以及知識豐富，但是我還沒抓到講話要領的其駿，有了你們的陪伴，研究生生活更加充實快樂！在這裡，也要跟我的戰友莞儒，說一聲謝謝和恭喜，我們一起面對考驗，也通過了，祝妳往後開心順利喔！

非常感謝羅竹芳老師和于宏燦老師，是你們協助我找到有興趣的研究主題，還有甲殼類病毒研究室的大家，實在太多人沒辦法一個一個感謝，大家都

對我很好，一起吃飯玩樂工作的日子，真的很開心！在那裡我也獲得許多，尤其是健宏學長的指導，讓我學會了各式各樣的實驗技術，很感謝。

無論什麼時刻，我最要感謝的是我的家人。感謝我有那麼好的爸爸，總是耐心和我對話，幫助我陪伴我成長。感謝媽媽，對於我的關心和鼓勵從不間斷，還會模仿和講笑話！並且辛勤工作提供我生活費，媽媽辛苦了。謝謝弟弟，常常打電話關心我或是送食物飲料來給我，謝謝你們，從你們眼中，我看到自己是最棒的。謝謝耕然，對你的感謝，說也說不完，謝謝你放假還陪伴我去實驗室，從來沒有一句埋怨，也一直是我最溫暖有力的依靠，讓我在疲憊失落的時候，有勇氣前進，謝謝你。我愛你們！

感謝一路上遇到的每一個人，我是多麼的幸運，才能有今天的成果。

最後，我要將這本論文，獻給我最親愛的奶奶，還有在天上的爺爺和外公。

摘要

在遺傳學的觀點上，種化基因指的是會造成物種間生殖隔離的基因。*Odysseus* (*OdsH*) 是第一個被發現，會造成果蠅的兩個姊妹種，擬黃果蠅和模里西斯果蠅的雜交雄性子代不孕的基因。根據DNA序列分析結果顯示，*OdsH*是由*unc-4*發生基因重複事件所產生，兩者都含有一個同源結構區，在黃果蠅種亞群中，擬黃果蠅和模里西斯果蠅的同源結構區有快速演化的現象。根據之前的研究顯示， 在黃果蠅中，*OdsH*主要表現在雄性成蟲的精巢，其功能被推測為藉由加速精子的生成率，以提高雄性的生殖率，但是到目前為止分子機制還不清楚。隨著技術的進步，果蠅的基因功能機制，可以利用UAS/Gal4系統，以異位表現的方式進一步分析。根據三個物種的*OdsH*在黃果蠅雌雄生殖系統表現的結果顯示，只有模里西斯果蠅的*OdsH*會造成雄性和雌性成蟲生殖器官發育異常，黃果蠅和擬黃果蠅的*OdsH*則不會。而當三個物種的*OdsH*在果蠅眼睛表現，都會造成嚴重的發育缺陷，造成小眼。根據胚胎以及幼蟲眼睛的觀察，當黃果蠅的*OdsH*表現時，會使得細胞週期受到干擾，並且是在細胞分裂期產生缺陷。因此，推測*OdsH*功能作用的分子機制為，參與細胞週期中的細胞分裂。結合最近在細胞株的觀察，發現*OdsH*可以結合到染色體中節的區域，*OdsH*在擬黃果蠅和模里西斯果蠅間造成的雄性子代不孕，可能符合centromere-drive model。

關鍵字：果蠅，*Odysseus*，基因重複，同源結構區，異位表現，細胞分裂。

Abstract

Genes that contribute to the reproductive isolation between species are known as "speciation genes'. *Odysseus* (*OdsH*) is a hybrid male sterility gene between *Drosophila mauritiana* and *D. simulans*. According to sequence analysis, *OdsH* duplicated from *unc-4* recently in the *Drosophila* genome preserving the intron exon structure and the paired-like homeodomain. Among *D. melaongaster* subgroup, the homeodomain of *OdsH* in *D. mauritiana,* and *D. simulans* evolved rapidly. Previous studies showed that *OdsH* is highly expressed in the testes, and the function of $OdsH^{mel}$ is to enhance male fertility by accelerating the rate of sperm maturation. Three *OdsH* alleles from *D. mauritiana*, *D. simulans*, and *D. melanogaster* were ectopically expressed in *D. melanogaster* with the Gal4/UAS system to uncover the molecular mechanism for the function of *OdsH*. In germline expression, $OdsH^{mau}$ caused developmental defect in the reproductive organs. Germline expression of $OdsH^{mel}$ in females caused the overlapping of nuclei in the embryos and embryonic lethality. In the eyes, all three alleles caused critical defect in the development resulting in small-eye phenotype. Results from embryos and eye discs indicate that cell cycle was perturbed at the mitotic phase with the expression of $OdsH^{mel}$. Therefore, the molecular mechanism of *OdsH* appears to play a role in the M phase of cell cycle regulation. Combined with the recent data in the cell culture indicating that *OdsH* can bind to pericentric satellite DNAs, the mechanism for *OdsH* to cause hybrid male sterility between *D. mauritiana* and *D. simulans* supports the centromere-drive model.

Keywords: *Drosophila*, *Odysseus*, gene duplication, homeodomain, ectopic expression, cell mitotic.

Contents

List of Tables

List of figures

Introduction

After the publication of “The Origin of Species”, the concept that all the life forms have evolved over time through the mechanism of evolution has become widely accepted. Nevertheless, the debate around the speciation developed into two theoretical concerns. First, how evolution initiates species evolution and second, how we define a “good” species? Those issues could only be discussed with the continued elaborating clarifying works upon the definition of species.

In Mayr’s biological species concept, he defined that “species are groups of actually or potentially interbreeding populations which are reproductively isolated from other such groups“ (Mayr 1963). Mayr's statement was the most widely applied concept among the existed species concepts. His proposed based on three advantages. First, closely related species with little distinguishable characters can be easily identified. Second, it can explain the existence of discontinuous phenotypes among sexually reproducing organisms. Moreover, the most important reason is that the researchers can immediately verify the existence of the subject (Coyne and Orr 2004).

In the biological species concept, the mechanism of isolation are particularly important, in which species of sexual organisms are defined as derived from reproductive isolation. Any biological difference or the reproductive characteristics between the populations that reduce gene exchange will cease gene flow between them and prevent species from fusing with another sibling species. There are many kinds of reproductive isolations, i.e. the pre-zygotic and the post-zygotic isolation. Most of the prezygotic isolations are resulted from the pre-mating isolation, while under the instances of postmating, prezygotic isolation may have happened on some species. In the genetic view of speciation, genes that contribute to the reproductive isolation are ‘speciation genes”, and most in the form of hybrid inviability or sterility.

The molecular mechanism for the speciation genes to cause reproductive isolation is interested.

Until now, several speciation genes in *Drosophila* had been studied, including *Hybrid male rescue* (*Hmr*), Na/K-ATPase alpha subunit isoform 2 (*JYAIpha*), *Nucleoporins 96* (*Nup96*), and *Odysseus* (*OdsH*). *Hmr* is the one in *Drosophila* causes hybrids incompatibility; *Hmr*, the X-linked gene in *Drosophila melanogaster*, encodes a rapidly evolving protein with the sequence similar to the myb/SANT-like domain in Adf-1 (MADF) class of DNA binding proteins, undergo functionally diverge between *D. melanogaster* and its sibling species (Brideau et al. 2009). Interspecific cross-mating of *D. melanogaster* females to the males of *D. simulans* resulted in lethality of the F1 hybrid males, because of the interaction between *Hmr* and the autosomal gene *lethal hybrid rescue* (*Lhr*), which localizes to heterochromatic regions of the genome in the *D. simulans*. *Lhr* also undergo to sequence diverged between these species.

JYAIpha was identified that resulting the hybrid sterility in *Drosophila*. *JYAIpha* encodes a protein, in which has a functional motif of an alpha subunit of a Na^+ and K^+ adenosine triphosphatase. The specific activating site involved in ion exchange, which is essential for the sperm motility. In *D. melanogaster*, *JYAIpha* is located in the fourth chromosome but translocated to the third chromosome in *D. simulans* lineage. Based on this long-term evolutionary transposition event, the hybrids males of *D. melanogaster* to *D. simulans* at last completely loss the *JYAIpha* gene and were sterile (Masly et al. 2006).

Nup96, which encodes a nuclear pore protein, was mapped as a hybrid inviability gene in hybrid males between *D. melanogaster* and *D. simulans*. In these two species lineage, *Nup96* evolved by positive selection, thus the *D. simulans* Nup96

protein is no longer compatible with the interacting factor that encoded by the *D. melanogaster* X chromosome. Later, another hybrid lethality gene nucleoporin Nup160kDa (*Nup160*) gene has been identified directly interact to *Nup96* (Presgraves et al. 2003; Tang and Presgraves 2009).

Odysseus (*OdsH*) is also the defined speciation gene that result in hybrid male sterility. The *OdsH* locus was noticed in hybrid sterility associated with three X chromosome regions in *D. mauritiana* and *D. simulans* hybrids, when the *D. mauritiana* allele introgressed into an appropriate *D. simulans* background (Coyne 1985). This sterility effect was closely linked to the *fork* (*f*) marker, and mapped the approximate location of this major effect hybrid sterility factor to 1.1cM on either side of *f* (Coyne and Charleswoth 1986). By ways of the chromosome introgression from *D. mauritiana* to *D. simulans*, the factor was further mapped between *f* and *Bx,* in cytological interval *16D* and namely *Odysseus* (*Ods*) (Perez et al. 1993). Result from a series of recombinants, the function of molecular factor in *Ods* were determined precisely. The longest fertile introgressions and the shortest sterile introgressions defined the minimized *Ods* gene within a genomic clone. Finally, *Odysseus* was cloned as a 340-amino-acid protein and predicted as a transcription factor with a paired-type homeodomain, a DNA binding motif, encoded by exon2 and 3 (Ting et al. 1998), therefore, it was named *OdsH* (for *Ods*-site homeobox gene). According to previous investigation, *OdsH* is known to be a duplicated gene from a neuron gene *unc-4*, and is 13-kb apart in tandem with it (Ting et al. 2004).

Both *OdsH* and *unc-4* consists of four exons with a paired-like type homeodomain on exons 2 and 3 sharing over 70% homology, and the structure of intron and exon are preserved (Ting et al. 2004). In *Drosophila*, both sequence and expression pattern of *unc-4* is conserved. In *Drosophila*, *unc-4* express in the

developing neuron system, female ovaries and male testes, while *OdsH* alleles are highly diverged not only in the sequential codon variation but also the expressing patterns among *D. melanogaster* subgroup including *D. mauritiana, D. melanogaster*, and *D. simulans* (Ting et al. 1998). *In situ* hybridization data showed that the *OdsH* is specifically expressed in the reproductive organs (Ting et al. 2004), and the expression pattern of *OdsH* in hybrids was mis-regulated (Sun et al. 2004). The functional studies in *D. melanogaster*, revealing that loss of *OdsH* would cause defect in male fertility at younger age, 2 to 4 days old, suggested that the normal function of *OdsH* is to enhance the fertility of young males by accelerating the sperm maturing (Sun et al. 2004). Furthermore, overexpression of *OdsH* has been shown to promote male fertility that more offspring production than wild type do, and the null mutant of *OdsH* can reduce the male fertility (Chen 2005). Therefore, the function of *OdsH* was suggested to accelerate the sperm maturation and enhance the fertility of the males.

Even there have several studies in the *OdsH*, now still need to gain more understand about the molecular mechanism for the function of *OdsH*, to solve the questions that how does *OdsH* play a role in spermatogenesis and what's the mechanism for *OdsH* to cause hybrid male sterile between *D. mauritiana* and *D. simulans*.

To address this question, ectopic expression - gene express in a place where it is normally inactive, is a powerful technique to gain further understanding of the gene function. In *Drosophila*, ectopic expression can be done by introducing a transgene with a modified promoter into the target organism or using the Gal4/UAS system. By ectopic expression tests with the UAS/Gal4 system, I want to do the analysis between three *OdsH* alleles, and to clarify the molecular mechanism of *OdsH* gene. Several Gal4 lines were chosen to induce three *OdsH* alleles expression in different tissues, by

crossing with *UAS-OdsH* constructs: *elav*-Gal4, expressed in the nervous system; *GMR*-Gal4, expressed posterior to the eye disc morphogenetic furrow (MF) in the third instar larvae; *nanos*-Gal4, expressed in male and female germline; and the ubiquitous expression line, *tub*-Gal4. In order to avoid the position effect in the expression analysis and to express the *OdsH* in the germline, the site specific transgenic vector that workable in the germline is necessary to be generated (Appendix I).

All of these ectopic expression lines give phenotypes. Among them, there are two lines deserve to do further analysis. The first one is the *nanos>OdsH* lines that have *OdsH* expressed in the place that similar to the endogenous expression. Second, the *GMR>OdsH* line, since *Drosophila* eye development is a process between cell division and differentiation such as the spermatogenesis in testes. It is desired that these experiment results will provide insight to the molecular mechanism of *OdsH* gene and the mechanism for *OdsH* to cause hybrid male sterility between *D. mauritiana* and *D. simulans*.

In addition to the molecular mechanism for the function of *OdsH*. As we have known that *OdsH* was duplicated from the *unc-4* gene. Find out the normal function of *OdsH* and *unc-4* will improve our understanding about the correlation between the duplication genes and speciation. *unc-4* was first isolated as a novel *Drosophila* pair-liked homeobox gene, DPHD-1, the homeodomain of DPHD-1 showed 85% amino-acid similarity to the *C. elegans* Unc-4 protein. *In situ* hybridization data of embryos and third-instar larvae revealed that the DPHD-1 mRNA is localized in subsets of postmitotic neurons in the central nervous system (CNS) and in the developing epidermis with a segmentally repeated pattern (Tabuchi 1998). In *Caenorhabditis elegans,* UNC-4 homeoprotein and Groucho-like corepressor UNC-37 were showed

function together in VA motor neurons to repress VB-specific genes that specify synaptic choice motor neuron circuit (Winnier et al. 2007). However, the normal function of the *unc-4* in the *Drosophila* is remained unknown. To comprehend the normal function, the microRNAs system in the *Drosophila* was applied to create the *unc-4* mutant (Appendix II).

In this study, the first aim is to reveal the molecular mechanism for the function of *OdsH*. To deal with this, three alleles of *OdsH* were analysis by ectopic expression examination. This may provide enlightenment in understanding the male hybrid sterility defect between *D. mauritiana* and *D. simulans.* Second, I want to identify the normal function of *unc-4* and to answer the question that whether *OdsH* have evolved novel function after the duplication event. With this, our understanding about these pair of duplication genes will be improved.

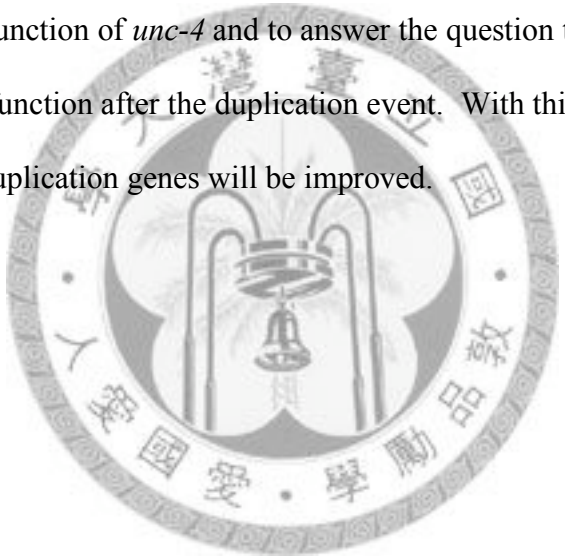

Materials and methods

Fly stocks

UAS-*OdsH*^{mel} line carrying *pP {5'-UAS::OdsH*^{mel}*}* construct was constructed by Yi-Lin Chen and Kah-Junn Tan (2005). Two attP insertion stocks, *ZH-attP-51D* (*y w* M{eGFP.vas-int.Dm}ZH-2A; M{*RFP.attP*}ZH-51D) and *ZH-attP-86Fa* (*y w* M{eGFP.vas-int.Dm}ZH-2A; +; M{*RFP.attP*}ZH-86Fa) were used to generate site specific transgenic lines (Bischof et al. 2007). Four Gal4 lines including *elav*-Gal4 *P{w*$^{+mW.hs}$ *=GawB}elav*^{C155} (Lin and Goodman 1994), *GMR*-Gal4: *w***; P{w*$^{+mC}$ *=GAL4-ninaE.GMR}12* (Freeman 1996), *nanos*-Gal4: *w*^{1118}; *P{w*$^{+mc}$ *=GAL4::VP16-nos.UTR}MVD1* (Van Doren et al. 1998), and *tub*-Gal4: *y*^{1} *w***; P{w*$^{+mC}$ *=tubP-GAL4}LL7/TM3, Sb*^{1} (Lee and Luo 1999) were obtained from the Bloomington stock center. The multiple balancer line, *w*^{1118}; *Cyo*/*Sp*; *TM3*/*Sb*, was used to set up the transgenic stocks. The His-2AvD GFP flies: *P{His2AvT;Avic/GFP-S65T}62A, Df*(*3R*)*nm136* were used for expression analysis (Clarkson and Saint 1999). All stocks were kept at 25°C and raised on the standard cornmeal medium.

Transgenic constructs

The cDNA fragments of *OdsH*^{sim} and *OdsH*^{mau} were digested from pBSKII (+)-*OdsH*^{sim} and pBSKII (+)-*OdsH*^{mau} by the restriction enzymes *Xba*I and *Kpn*I, and subcloned into the transgenic vector *pUASP attB*. The transgenic constructs were named *pP{5'-UAS::OdsH*^{sim}*}* and *pP{5'-UAS::OdsH*^{mau}*}* respectively (Fig. 1).

Transgenic lines

Two constructs *pP{5'-UAS::OdsH*^{sim}*}* and *pP{5'-UAS::OdsH*^{mau}*}* with attB site, were microinjected into *ZH-attP-51D* and *ZH-attP-86Fa* respectively (thanks for help of Chiou-Yang Tang). After homozygous transgenic stocks were established on

the second or third chromosome, the transgenic flies were crossed to different Gal4 lines (Fig. 2 and Fig. 3).

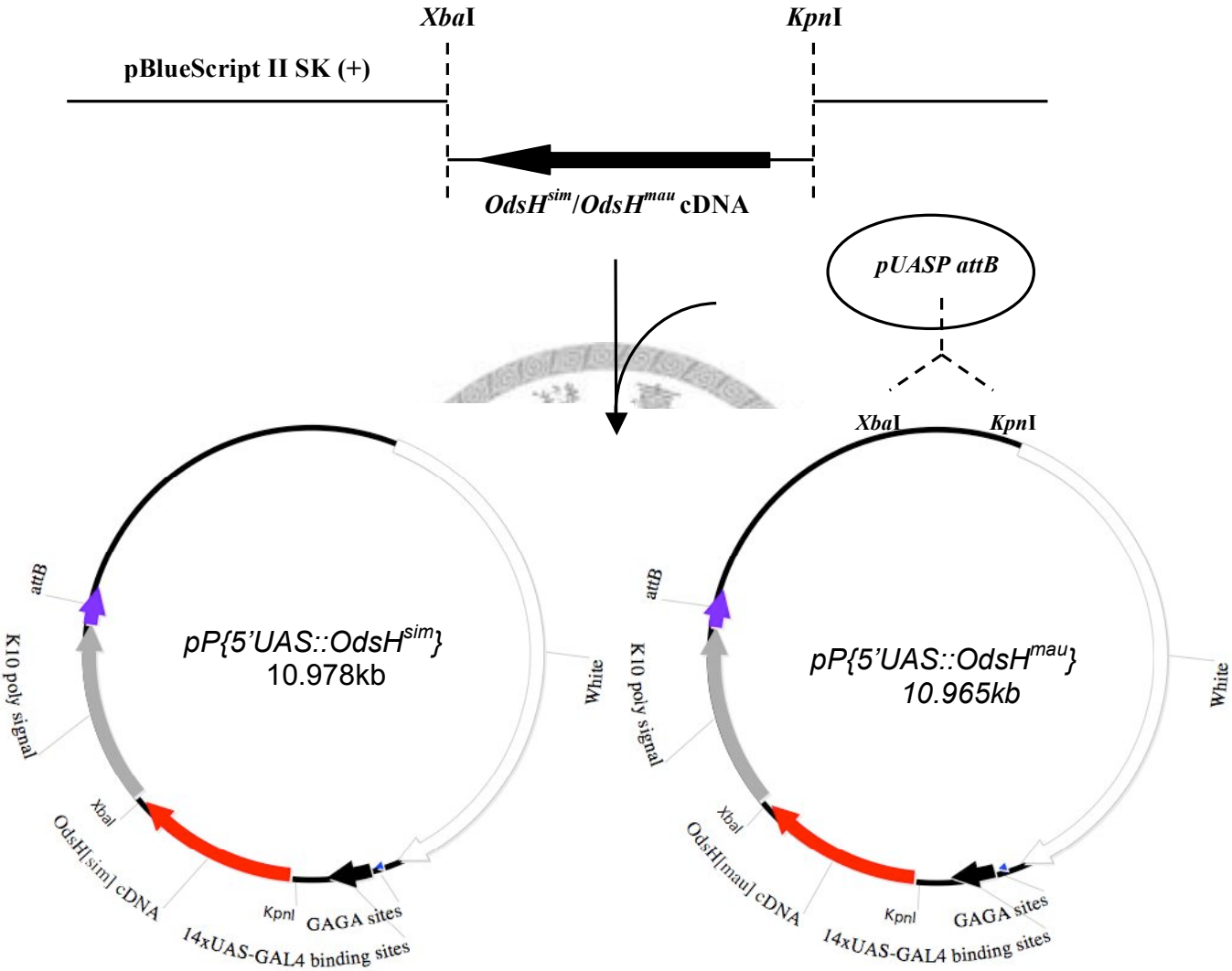

Fig. 1.—Procedure of *pP{5'-UAS::OdsH^{sim}}* and *pP{5'-UAS::OdsH^{mau}}* constructs. Dashes mean the digestion by the nearby restriction enzymes. The cDNA of *OdsH^{mau}* and *OdsH^{sim}* were cut out with *Kpn*I and *Xba*I from the vector pBluescript II SK(+) and cloned into the site specific integration vector *pUASP attB* to get the UAS constructs.

injection
↙
G0 male or female x w^{1118} male or female
↙
G1 **select red-eyed flies** double balancer male or female
+/*P* ; +/+ x *CyO*/*Sp* ; *TM3*/*Sb*
male or female
↙↘
G2 **select flies with CyO marker** x *CyO*/*P* ; *TM3*/+
CyO/*P* ; *TM3*/+ male or female
male or female
↙↘
G3 **select flies without CyO marker** x different Gal4 lines
P/*P* ; +/+
male or female male or female
↓
For ectopic expression analysis

Fig. 2.— The cross steps to get ectopic expression line on second chromosome.

injection
↙
G0 male or female x w^{1118} male or female
↙
G1 **select red-eyed flies** double balancer male or female
+/+ ; +/*P* x *CyO*/*Sp* ; *TM3*/*Sb*
male or female
↙↘
G2 **select flies with TM3 marker** x +/*CyO* ; *TM3*/*P*
+/*CyO* ; *TM3*/*P* male or female
male or female
↙↘
G3 **select flies without TM3 marker** x different Gal4 lines
+/+ ; *P*/*P*
male or female male or female
↓
For ectopic expression analysis

Fig. 3.—The cross steps to get ectopic expression line on the third chromosome.

RNA extraction

For the total RNA extraction, 0-5 day-old adult flies were collected. Before RNA extraction, flies were put into an empty vial to void most of yeast for at least 2 hours. Total RNA was extracted with the TRIzol® reagent followed the manufacturer's instructions (Invitrogen). The extracted RNA were then treated with the DNase for 15 min at 25°C. After inactive the DNase by the EDTA for 10 min at 65°C, RNA was reverse-transcribed. The left RNA was stored in DEPC water at -80°C.

RT-PCR

For Reverse Transcription (RT), 5μg total RNA was used as the template for cDNA synthesis. The SuperScript II First-Strand Synthesis system with a mixture of Oligo-dT (Invitrogen), dNTPs (10 mM), RNA (5 μg), and DEPC- ddH_2O was incubated for 5 min at 65°C. The RT contents were collected at the bottom by centrifuging, and 5X RT buffer, 25mM $MgCl_2$, 0.1 M DTT, RNAse OUT™, Superscript II RT were added. For PCR reactions, the reactions contained 8ng template, 1X reaction buffer, 1.5mM $MgCl_2$, 16nM dNTP, 1 unit Taq polymerase, and 40nM primers each in a final volume of 20μl were amplified for 30 cycles of 30s at 95°C, 30s at 58°C, 1min 20s at 72°C, and the final extension at 72°C for 7min. The PCR amplification products were analyzed by electrophoresis in 1.5% agarose gels. *Drosophila* ribosomal protein 49 encoding gene (*rp49*) was used as a loading control for the PCR reactions. Gene specific and *rp49* primers for RT-PCR were listed in Table 1.

Table 1
The list of primers for expression analysis.

Gene	Primer	Direction[1]	Sequences
rp49	rp49F	F	5'CAGTCGGATCGATATGCTAAGCTGT3'
	rp49R	R	5'TTACCGACCTTGGGCATCAGATACT3'
OdsH	OdsH c0^{+}	F	5'GCAAAAGCTAAGACGAAAATGGAT3'
	U8 4524-	R	5'TGCTTAGCTAACCACCCGAAATCA3'
unc-4	unc-4-552+	F	5'AGCCCGTCGTCGAAAGAAGC3'
	unc-4-739-	R	5'TTCGCCCTCGTCGTCGCTGTC3'

[1]"F", forward primers; "R", reverse primers.

Embryo collection

Adult flies were transfer into a plastic bottle with a grape juice agar plate. The prelaying time is 45mins each twice. After prelaying, change new plate for collecting embryos. Embryos were collected from the grape juice agar plate with dH_2O into a Nitex nylon mesh (Cat. 3-100/47, Tetko Inc) and dechorionated with 50% bleach for about 5mins. These dechrionated embryos were washed with dH_2O again and transfer into a glass bottle containing 1:1 n-heptane: 4 % paraformaldehyde for 20-30min fixation. Remove the bottom aqueous layer, and add 100% methanol with the same volume and shaked for 1 min vigorously. The devitellinized embryos will at the bottom of the bottle. Remove the heptane and wash several times with 100% methanol. Embryos can be stored in the methanol and kept in -20°C (Theurkauf 1992).

Testes and ovary dissection

To observe the reproductive organs, the testes and ovaries were dissected in the 1XPBS, and fixed in the 2% Glutaraldehyde (Sigma) for 5min. After this, mounting samples onto the glass slide in 1XPBS solution (White-Cooper et al. 1998). Pictures were taken with the fluorescent microscopy: Zeiss Axio Imager A1.

Scanning electron microscopy (SEM)

Adult flies were fixed in 70% ethanol for 1hr, dissecting the heads dehydration. Incubated the heads in serious dilution ethanol, including 85%, 90%, and 95% ethanol for 30mins each. Wash with 100% ethanol twice for 30mins each and acetone twice for 30mins each. Samples are dried after treating in critical point dry (CPD) specimen. After mounting samples on the studs, put them into the chamber of the sputter coater and coated with a thin golden film (Domínguez et al. 1998). These eyes were examined by a scanning electron microscope: FEI INSECT S. and images were acquired using the xT microscope server software.

Immunostaining

Dissecting eye-antennal discs from third instar larvae in 1X PBS, then transfer into fixation solution (4% paraformaldehyde in 1X PBS) for 15mins at room temperature. Washing the fixed eye-antennal discs with 1XPBST (1X PBS+ 0.3% Triton-100) three times for 5 mins each, then incubate in the 1XPBST contain 3% BSA with rabbit anti-phosphohistone H3 (1:800) or rat anti-elav (1:500) antibody overnight at 4°C. Following, the samples were washed with 1X PBST three times and incubated with secondary antibodies conjugated with either FITC or Rodamin for 2hrs in dark at room tempterture. The discs were then washed 3 times with 1X PBST before mounting (Pai et al. 1998).

To label the S phase cell at the second mitotic wave, eye discs were dissected in 1XPBS and incubated in PBS containing 0.1 mg/ml of Bromodeoxyuridine (BrdU) for 40 mins. Discs were fixed with 4% para-formaldehyde for 30 mins, then treated with 3N HCl for 15 mins. After washing by PBST for three times and incubated with mouse anti-BrdU antibody in PBST containing 3% bovine serum albumin (BSA) at

4°C overnight, the BrdU signal was detected by secondary antibodies conjugated with FITC (Secombe et al. 1998).

All discs were mounting discs on the glass slide with their apical face up in mounting solution and pictures were taken with a confocal spectral microscope system: Lsica TCS SP5 and the LAS AF software.

Results

The *OdsH* transgenic lines

In order to study the molecular mechanism of the *OdsH*, set up *OdsH* transgenic flies for the subsequent ectopic expression analysis. Flies carrying UAS-$OdsH^{mel}$ construct was created by Yi-Lin Chen, and $OdsH^{sim}$ and $OdsH^{mau}$ each were cloned into the *pUASP attB* transgenic vector for germline expression. *pP{5'-UAS*::$OdsH^{sim}$*}* was injected into 29 embryos for each attP lines, and 11 larvae of *ZH-attP-51D* and 17 larvae of *ZH-attP-86Fa* were collected. Finally, one transformant on the second chromosome and three transformants on the third chromosome were obtained. For *pP{5'-UAS*::$OdsH^{mau}$*}*, 30 embryos were injected for each lines and 11 larvae of *ZH-attP-51D* and 17 larvae of *ZH-attP-86Fa* attP lines were collected. Only one transformant of each chromosome was obtained (Table 2). The third chromosome insertion lines for each UAS construct was used to cross with different Gal4 lines for ectopic expression analysis.

Table 2
The list of *UAS-OdsH* transgenic lines

	Numbers of injected embryo	Numbers of hatched larvae	Transformant
UAS-$OdsH^{sim}$			
ZH-attP-51D	29	11	1
ZH-attP-86Fa	29	17	3
UAS-$OdsH^{mau}$			
ZH-attP-51D	30	11	1
ZH-attP-86Fa	30	17	1

Ubiquitous and neuron expression of *OdsH* alleles

According to previous investigation. *OdsH* is known to be a duplicated gene from a neuron gene *unc-4*. Expression sites of *unc-4* can be in neuron cells, female ovaries and male testes. However, *OdsH* is notified highly expressed in testes but not

in neuron cells or female ovaries (Ting et al. 2004). Divergence function of *OdsH* from *unc-4* is still unknown. In order to understand the molecular mechanism for the function of *OdsH*, different *OdsH* alleles from the *Drosophila* species: *D. mauritiana*, *D. melanogaster*, and *D. simulans* were overexpressed at several specific tissues by the UAS-Gal4 system here, and the result is showed in Table. 3.

Table 3
Phenotypes of ectopic expression of *OdsH* alleles.

	Expression site	UAS-*OdsH*^{mel}	UAS-*OdsH*^{mau}	UAS-*OdsH*^{sim}
elav-Gal4	neuron cell	embryonic lethal	no defect	no defect
GMR-Gal4	eye disc	small and smooth eye	small and rough eye	small and rough eye
nanos-Gal4	germ line cell	Female sterile (maternal effect embryonic lethal) male fertile	female and male sterile	female and male fertile
tub-Gal4	ubiquitous	larval stage lethal	no defect	no defect

First I used *tub*-Gal4 to drive three *OdsH* alleles for ubiquitious expression. The phenotype of flies with *tub>OdsH*^{mel} showed larval stage lethal. In addition, I used *elav*-Gal4 to make the *OdsH* alleles expressed in neuron cells. In *elav>OdsH*^{mel}, all offspring died at the embryonic stage and no larvae and adults could be observed. These results indicated that misexpress of *OdsH* would influence the early stage development of *Drosophila*.

In addition to the effect of *OdsH*^{mel}, *OdsH*^{mau} and *OdsH*^{sim} were also analysis by two Gal4 lines, *tub*-Gal4 and *elav*-Gal4. Both the expressions of *OdsH*^{mau} and *OdsH*^{sim} have no clear effects in the developmental process and many adult flies can be obtained.

Germlines expression of *OdsH* alleles

OdsH is a rapid evolved gene that the amino acid is highly diverged among *D. mauritiana, D. melamogaster*, and *D. simulans*. The endogenous *OdsH* is highly expressed in the male reproductive system, but loss of the expression in the female germline where is one of the expression site of *unc-4*. Here, I analyzed the influence of *OdsH* in both male and female germlines by using *nanos*-Gal4. Morever, it is also interesting to investigate the sequence divergence of the *OdsH* alleles in the germline system of *D. melanogaster*.

In order to check the germline expression by using the site specific transgenic vector *pUASP attB*, which I have modified from the *pUAST attB*. *OdsH* expression was detected by RT-PCR. Primers specific for *OdsH* were used. The result showed that *OdsH* was expressed in the females which carry either *nanos*> $OdsH^{sim}$ or *nanos*> $OdsH^{mau}$ but no expression in the females from w^{1118} (Fig. 4). Therefore, the vector *pUASP attB* was successful to induce gene expressed in female germlines.

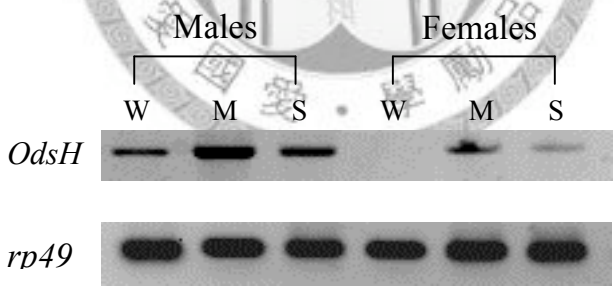

Fig. 4.—RT expression of *OdsH* in males and females. Males RNA were extracted from three different lines, including w^{1118} (w), *nanos*>$OdsH^{mau}$ (M), and *nanos*>$OdsH^{sim}$ (S). While in females, only the flies with *OdsH* overexpression in germline cells have the *OdsH* product after RT-PCR procedure. *rp49* was used as the control gene in all samples.

Females from three *nanos*>*OdsH* lines showed different phenotypes. *nanos*>$OdsH^{mel}$ led to sterile phenotype of females, but the morphology of the ovary looked similar to the one from the w^{1118}. Females with $OdsH^{mel}$ expression in the germline have normal form egg chamber, which contains ovum in various stages.

More specifically, female manage to lay eggs, but all of them died at the embryonic stage. Females with *OdsH*^{sim} expressed in germlines have no clear defect in fertility. The morphology of egg chambers in the ovaries are also normal. However, females with *OdsH*^{mau} expressed in germlines are sterile and cannot produce embryos. Observation the ovaries dissected from these females under the microscope showed that they are much smaller than those in the adults carrying *UAS-OdsH*^{mel} and *UAS-OdsH*^{sim} (Fig. 5).

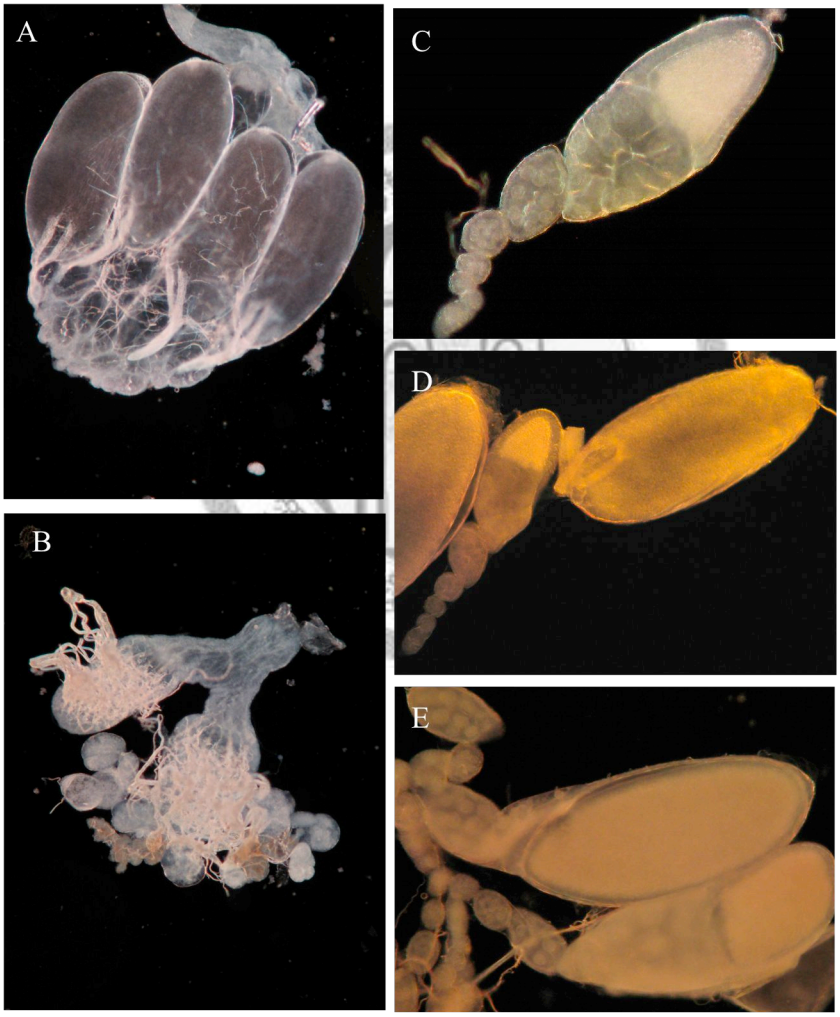

Fig. 5.—Gal4 inducible expression in the germline of the ovary. (A) The ovary from w^{1118} contains many egg chambers in it, and every female has two ovaries in the abdomen. The morphology of ovaries from females carrying with *nanos>OdsH*^{mel} and *nanos>OdsH*^{sim} are similar to w^{1118}. (B) In *nanos>OdsH*^{mau} famels, there are two ovaries can be seen but the size of the ovaries are much smaller than that in w^{1118}. Besides, the structure are abnormal that without any egg chambers. Various stages of the ovum can be seen in the egg chambers from the ovaries of the females in w^{1118} (C), in *nanos>OdsH*^{sim} (D), and in *nanos>OdsH*^{mel} (E).

To figure out the defect in development leading to embryonic lethality in *nanos>OdsH*^{mel} line, females with *nanos>OdsH*^{mel} genotype were allowed to lay eggs for 30 minutes, and the embryos were collected. In general, embryos would go through the syncytial blastoderm stage at about 1hr 30min to 2hr 30min. In this stage, the nuclei in the embryos will divide four or more times syncytially. Immediately after the last division, the nuclei migrate to the surface and begin to partition into individual cells. Thus, when collecting the wild type embryos at 1 hr 30min, the individual nuclei can be seen clearly and the nuclei spaced evenly. Following this stage, cells are going to gastrulation. Through microtubles dynamics the archenteron is formed. This structure can be seen when wild type embryos were collected after 3hrs development. However, while checking the embryos morphology under the microscope, nearly 50% of the embryos have uneven yolk distribution. There were parts in these embryos without yolk. The distribution of yolk among them were irregular, unlike to the morphology of wild type embryos (Fig. 6). With the uneven yolk distribution, the embryos failed to develop and showed embryonic lethal.

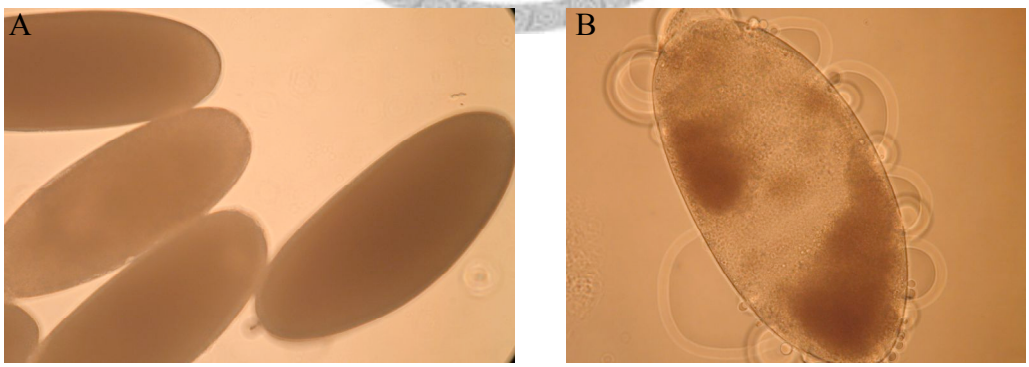

Fig. 6.—The morphology of the early embryos. Embryos were collected in 30min. (A) In w^{1118}, all the embryos have even yolk distribution under microscope. (B) In *nanos>OdsH*^{mel} , nearly 50% of the eggs produced from the females, with *OdsH*^{mel} expressed in germline, have uneven yolk distribution. Part of the eggs are empty under microscope.

When the nuclei of the embryos were labeling by GFP, with the homozygous line of *nanos>OdsH*^{mel} crossed to the His-2A GFP flies, the signal indicated that the nuclei are not spaced evenly. Many of the nuclei overlap with each other (Fig. 7). Additionally, very high percentage of the mutant embryos could not form the archenteron successfully and caused a twisted phenotype (Fig. 8).

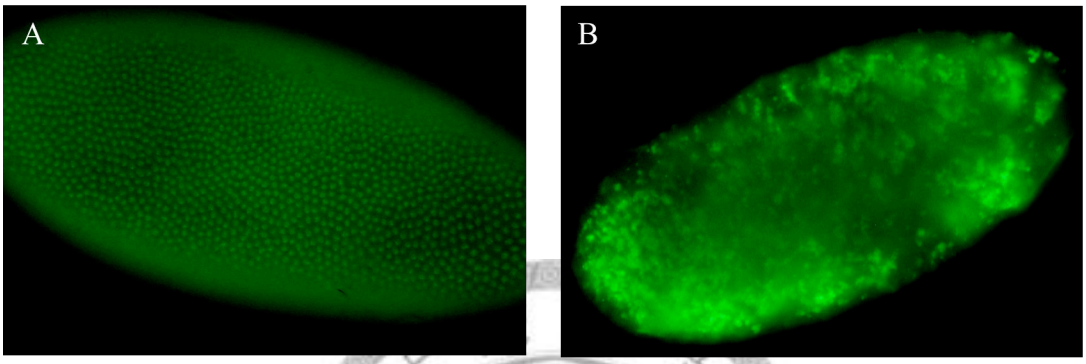

Fig. 7.—Nucleus pattern in the embryos. Embryos were collected in 1.5hr from: w^{1118} and *nanos>OdsH*^{mel}. (A) In w^{1118}, the embryos are at the late time of the syncytial blastoderm (about stage 4) and begin moving into the cellularization stage. Under the microscope, the individual nuclei are visible and distribution uniform. (B) In the embryos from the females with *nanos>OdsH*^{mel}, the individual nuclei cannot be seen clearly since they overlap to each other.

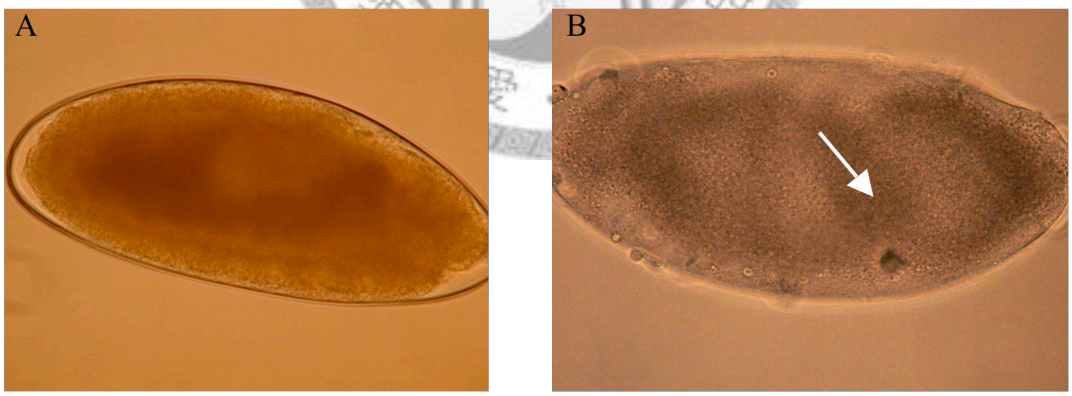

Fig. 8.—Embryos in the gastrulation stage. Embryos were collected in 3hrs from: w^{1118} and *nanos>OdsH*^{mel}. (A) In w^{1118}, the gastrulation stage of the embryos begin as soon as the cell formation finish, and form the structure of the archenteron. (B) In the embryos collected from the females with *nanos>OdsH*^{mel}, the force from the microtubules dynamic cannot induce cell migration to form archenteron structure successfully and result in twist phenotype. Arrow shows the twist part in the embryo.

Males in *nanos>OdsH*^{mel} and *nanos>OdsH*^{sin} lines do not appear to have reproductive defects with the ability to produce offspring and both the testes and accessory gland structures were normal when compare to w^{1118}. On the contrary, when males carrying *nanos>OdsH*^{mau} cross to the w^{1118} females, there were no larvae due to the embryonic lethal phenotype. Besides, there are critical defect in the testes development with *OdsH*^{mau} expression (Fig. 9).

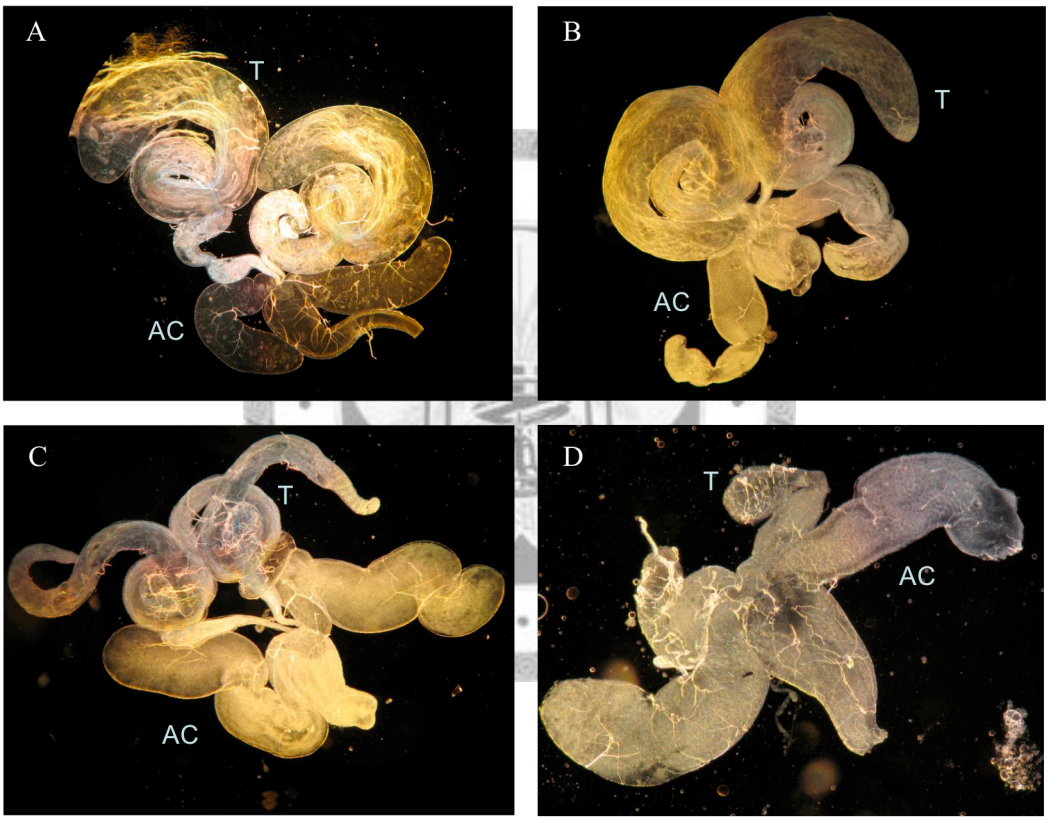

Fig. 9.—The morphology of the male reproductive organ. Dark field of the male germline tissue. The testes (T) and accessory gland (AC) structures are clear to be seen in (A) w^{1118}, (B) *nanos>OdsH*^{mel}, and (C) *nanos>OdsH*^{sim}. While the testes wither in all the males of *nanos>OdsH*^{mau} in (D).

Eye disc expression of *OdsH* alleles

Drosophila eye development involves cell division and differentiation similar to spermatogenesis in the testes where *OdsH* is normally expressed. In addition, many signaling pathways that regulate eye development are well identified. According to the observation in germline that the expression of $OdsH^{mel}$ in female germlines would cause embryonic lethal with the abnormal nuclei pattern. *Drosophila* eye was applied to test whether *OdsH* plays a role in cell cycle regulation. *GMR*-Gal4, which expresses posterior to the morphogenetic furrow in the eye discs of the third instar larva, was chosen to drive *OdsH* alleles expression.

Morphology of adult eyes

The transgenic flies with *UAS-*$OdsH^{mel}$ were crossed to *GMR-Gal4* to induce the expression of *OdsH* during eye development. All the eyes of these flies have smaller size than the normal eye and have shuttle-liked phenotype. Besides, the eye surface is very smooth when compared to the three-dimensional compound eye structure in the w^{1118}, as the control line. According to the Scanning electron microscopy (SEM) pictures, the hexagon ommatidia that form the compound eye with uniform disturbed bristles were clear to be seen, and the width of the eye was measured. The width range of the eye from w^{1118} is 334 μm and decrease severely to 175 μm in the adults with *GMR>*$OdsH^{mel}$. Flies carrying homozygous *OdsH* expression in the eye discs, the eye size will be reduce to 133 μm. In addition, there are not any ommatidia structures and fewer bristles contained in both heterozygous and homozygous lines (Fig. 10B and 10C).

In addition to the $OdsH^{mel}$, the defects induced by different alleles of *OdsH* were also observed in the eye development. Driving $OdsH^{mau}$ and $OdsH^{sim}$ expression by *GMR*-Gal4 in the larva eye discs also showed the critical eye phenotypes. Both of

the eyes from *GMR>OdsH*^{mau} and *GMR>OdsH*^{sim} are smaller than normal ones. Under the SEM, mean width of the eye been measured is about 224 μm from *GMR>OdsH*^{mau} and 207 μm of the eye from *GMR>OdsH*^{sim}. Both two alleles of *OdsH* cause the eyes become rough and lose the ommatidia structure. Some individuals showed few bristles and some individuals have no bristles. Thus, the eye size is smallest with *OdsH*^{mel} expressed in the third instars larva eye discs when comparing to the eye from *GMR>OdsH*^{sim} and *GMR>OdsH*^{mau} (Fig. 10). Additionally, size of the eyes showed a different level decrease in three different *GMR-OdsH* lines (Fig. 11).

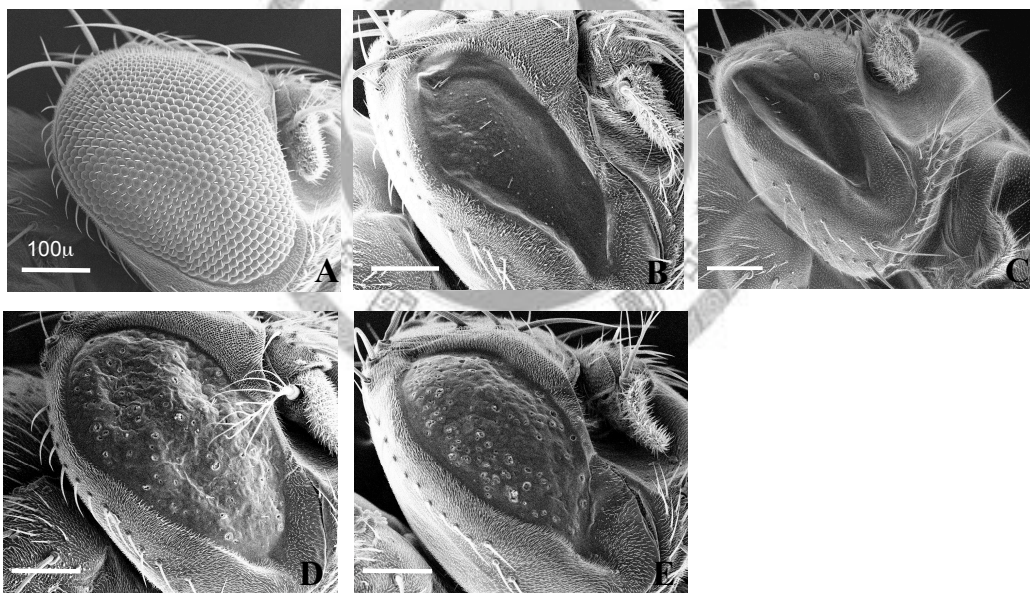

Fig. 10.—The morphology of adult eye with ectopic expression different alleles of *OdsH*. The eye typr in (A) *w*^{1118}, (B) *GMR>OdsH*^{mel} heterozygous strain, (C) *GMR>OdsH*^{mel} homozygous strain, (D) *GMR>OdsH*^{mau}, and (E) *GMR>OdsH*^{sim} are showed in SEM. Scale bar = 100μm.

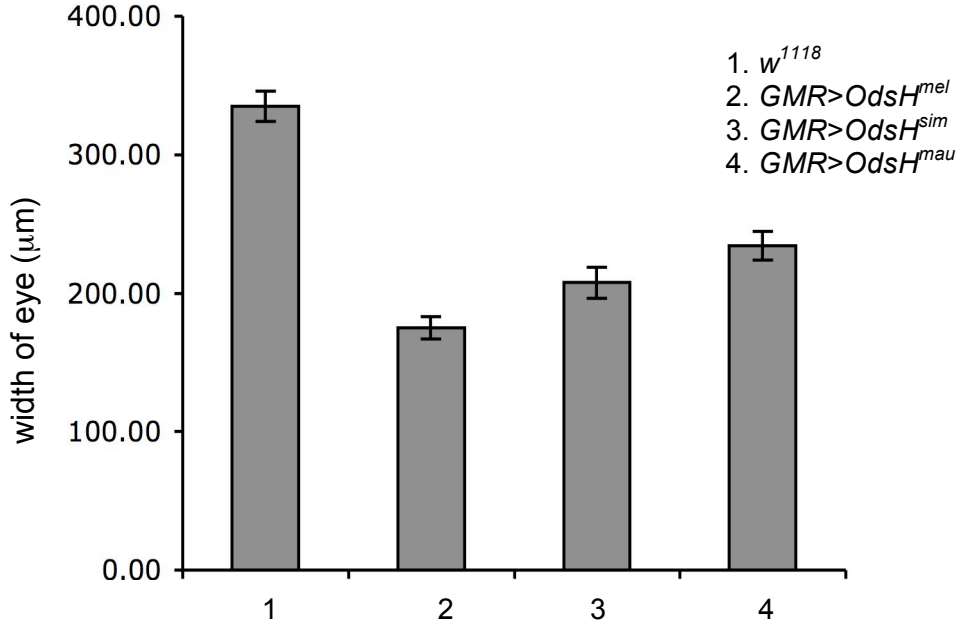

Fig. 11.—The width of eye with different *OdsH* alleles expressed. Bar graph showing the width of adult eyes with *OdsH* express (mean ± SE). The mean value in w^{1118} is 334μm, 175μm in *GMR>OdsH*^{mel}, 207μm in *GMR>OdsH*^{sim}, and 224μm in *GMR>OdsH*^{mau}. All the statistical analysis were compared to *GMR>OdsH*^{mel} (Student's t-test, $P<0.05$).

The influence of *OdsH*^{mel} in mitotic cells

According to the observation in the critical eye phenotype that caused by the ectopic expression of *OdsH*^{mel}, I did the antibodies staining to see whether it was a consequence of the defect in the cell-cycle regulation. Neuron clusters and mitotic cells were detected by anti-Elav and anti-phosphohistone3 antibodies. Elav is to detect the neuron clusters and phosphohistone3 can label the cells that undergo mitosis. Comparing the eye discs from w^{1118} and *GMR*;*OdsH*^{mel}, the mean columns and arrangement of the neuron clusters are not significant different. For my results, the mitotic cell numbers at the second mitotic wave (SMW) that posterior to the morphogenetic furrow were increase in *GMR>OdsH*^{mel} (Fig. 12). The cell numbers at the SMW of the eye discs from *GMR>OdsH*^{mel} contained about 65 (n=30) and there are about 51 cells (n=19) in the disc from w^{1118}. According to the Student's t-test, they showed statistically significant difference (Fig. 13).

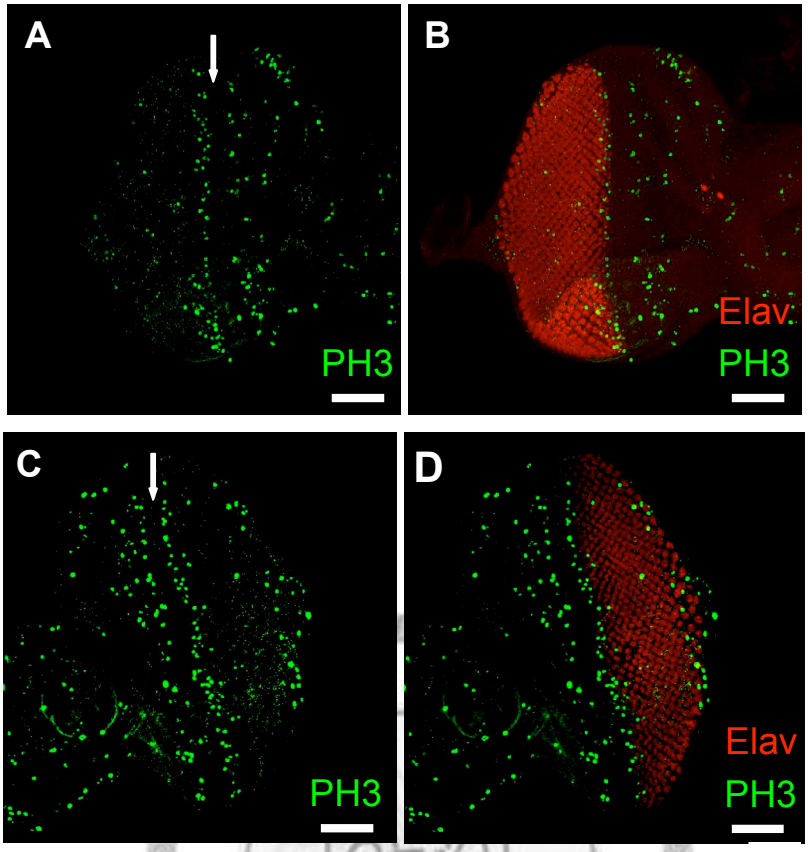

Fig. 12.—The mitotic cell with *OdsH*^{mel} expression. Anti-phospho-histone H3 antibody labeled the mitotic cells at the first and second mitotic wave, and anti-Elav antibody revealed the neuron clusters. The mitotic cell number at second mitotic wave in (A-B) w^{1118}, and were increased in (C-D) *GMR;OdsH*^{mel}. Arrows indicated the furrow. Scale bar = 50 μm.

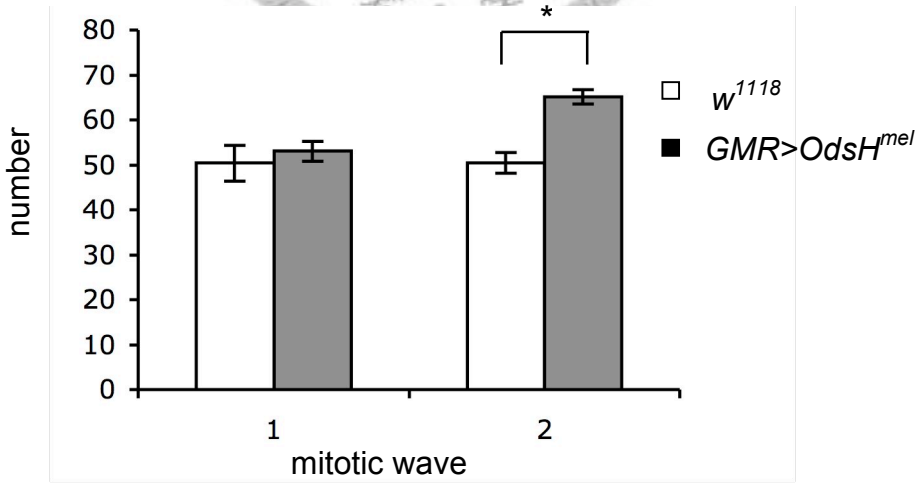

Fig. 13.—Quantification of the mitotic cells at the first and second mitotic waves. Bar graph shows the mitotic cell numbers (mean ± SE) at the second mitotic wave in the w^{1118} and *GMR>OdsH*^{mel}. The mitotic cell numbers at the second mitotic wave are significant different between two lines (Student's t-test, P<0.0001).

The increase of the mitotic cells at the SMW could be due to the mitotic defects that happened in the SMW to cause the accumulation of arrested mitotic cells poster to the morphogenetic furrow, or multiple rounds of cell division occurring poster to the furrow. In order to distinguish between these two hypothesis, Bromodeoxyuridine (BrdU) which is synthetic thymidine analog that can replace the space of thymidine and incorporated into the replicating DNA was applied to label the S phase cells at the SMW. The distribution and the number of the BrdU-labeling cells are similar between w^{1118} and *GMR>OdsH*^{mel} (Fig. 14). This result indicated that there are not more cells undergoing multiple rounds of cell division in *GMR>OdsH*^{mel}, and the mitotic cell numbers increase in the *GMR>OdsH*^{mel} was caused by the mitotic defect.

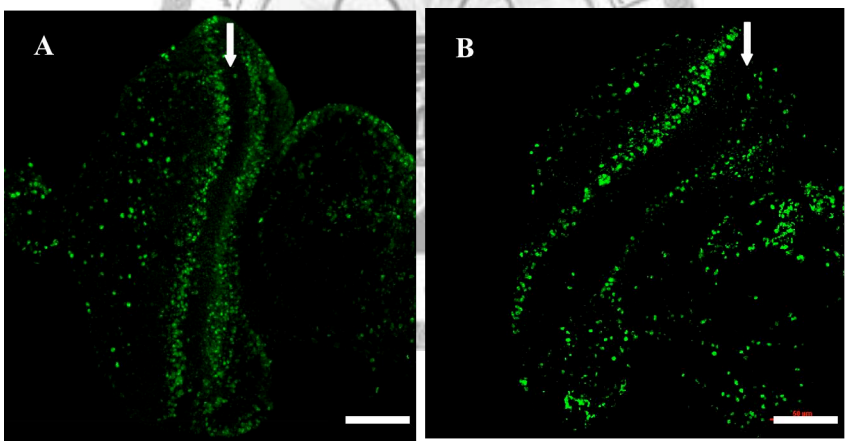

Fig. 14.—S phase cell in third-instar larva eye disc. The cells were labeled with anti-BrdU antibody at the SMW in (A) w^{1118} and (B) *GMR>OdsH*^{mel} eye discs. Arrows indicated the morphogenetic furrow. Scale bar = 50 μm.

Discussion

In order to gain more insight in the molecular mechanism for the function of *OdsH* and find out the possible mechanism of the hybrid male sterility between *D. mauritiana* and *D. simulans*. Ectopic expression analysis by the UAS/Gal4 system was applied. The site specific transgenic vector that was workable in the germline cells and named *pUASP attB* were generated first. This vector overcomes two limitations for the original transgenic vector *pUAST*: the insertion of the UAS construct is random that would have the position effect in the phenotypic analysis, and the activity of *pUAST* is poorly in the germline (Brand and Perrimon 1993). The modified vector called *pUASP* were generated and was shown to drive efficient expression in germline (Grossniklaus et al. 1989; Spardling 1993), but it still have the problem with the random insertion. The *pUASP attB* vector, which I have generated here was modified from the site specific transgenic vector called *pUAST attB* (constructed by Johannes Bischof and Konrad Basler). The UAS constructs made with *pUASP attB* will have the specific integration site in the *Drosophila* genome when injected into the attP lines, by the recombination between the attB sequence in the vector and the attP sequence in the *Drosophila* genome (Fish et al. 2007). In site specific integration, the genome mapping procedure to check the insert site is necessary, additionally, it can avoid the position effect when comparing different insertion lines. Second, *pUASP attB* works well in germline cells that it contains the important motifs from the traditional germline cells workable transgenic vector *pUASP*. UAS constructs with different alleles of *OdsH* in three *Drosophila* species including *D. melanogaster, D. simulans,* and *D. mauritiana* were then generated.

According to the ectopic expression analysis, the overexpression of *OdsH* in developing neuronal cells during early embryonic stage result in embryonic lethal, but

this defect were not observed in the *elav>OdsH*^{sim} or *elav>OdsH*^{mau} embryos. In the germline expression, the *OdsH* allele from *D. mauritiana* caused defects of the reproductive organs and result in male and female sterility, while *OdsH*^{sim} have no effect in the development of the testes and the ovaries. The females with *OdsH*^{mel} expression were sterile with the embryonic lethal phenotype, but males with *OdsH*^{mel} expression were fertile. In *Drosophila* eye development, all three alleles of the *OdsH* expression caused the decrease in the eye size with the gradient difference. The immunostaining results show that the mitotic cells were interfered with the *OdsH*^{mel} expression.

***OdsH* in *D. melanogaster* germline cells**

The expression of the *OdsH* allele from *D. mauritiana* causes the reproductive organs in both males and females withered in the *D. melanogaster* genetic background, and there were no gametes produced. However, this phenotype was not appearing in the flies that expressed *OdsH* alleles from *D. melanogaster* or *D. simulans*. These results suggested that the *OdsH* allele of the *D. mauritiana* is largely different from it in *D. melanogaster* and *D. simulans*.

OdsH, which contains two important motifs including homeodomain and Engrailed homology 1 (Eh1) domain, is a rapidly evolving gene that the sequences are highly diverged among *D. mauritiana*, *D. melanogaster*, and *D. simulans* (Ting et al. 1998). Among diverse texa, homeodomain is very conserved, but according to the sequence alignment of the *OdsH* alleles in the three species, many amino acids subtitution between three species. In the *OdsH*^{mau}, there are eight amino acids different from *OdsH*^{mel} and *OdsH*^{sim}. Among these eight amino acids, four residues have changed the polarity, residues 152 and 157 have become non-polar amino acid, and residue 196 changed to the polar amino acid. This property is important in

protein structure and protein-protein interaction. Therefore, these amino acids can be the candidates contribute to the different phenotype in germline expression. On the other hand, Engrailed homology 1 (Eh1) domain may be another possible region to cause the variance.

Among *Drosophila* species, the Eh1 domain is conserved, *OdsH* from *D. mauritiana* has a premature stop codon resulting in the loss of the Eh1 domain function (Fig. 15). Eh1 domain is the repression domain first identified in the *Drosophila* Engrailed homeodomain protein, and it has been reported to interact with Groucho protein (Riz et al. 2009). Groucho proteins are widely expressed nuclear factors, which have no DNA-binding activity. By interacting with DNA-binding factor to influence its function, many patterning and differentiation events of the development are regulated (Buscarlet and Stifani 2007).

To synthesize, according to the phenotype of germlines expression and the information from the sequence alignment between *D. melanogaster*, *D. simulans* and *D. mauritiana*. There are three possible regions in $OdsH^{mau}$ to play important roles in the function of *OdsH* to affect the fertility in the *D. melanogaster* genetic background. Furthermore, result in the developmental defect of the reproductive organs. The regions are: seven amino acids substitution in the homeodomain, and the Eh1 domain.

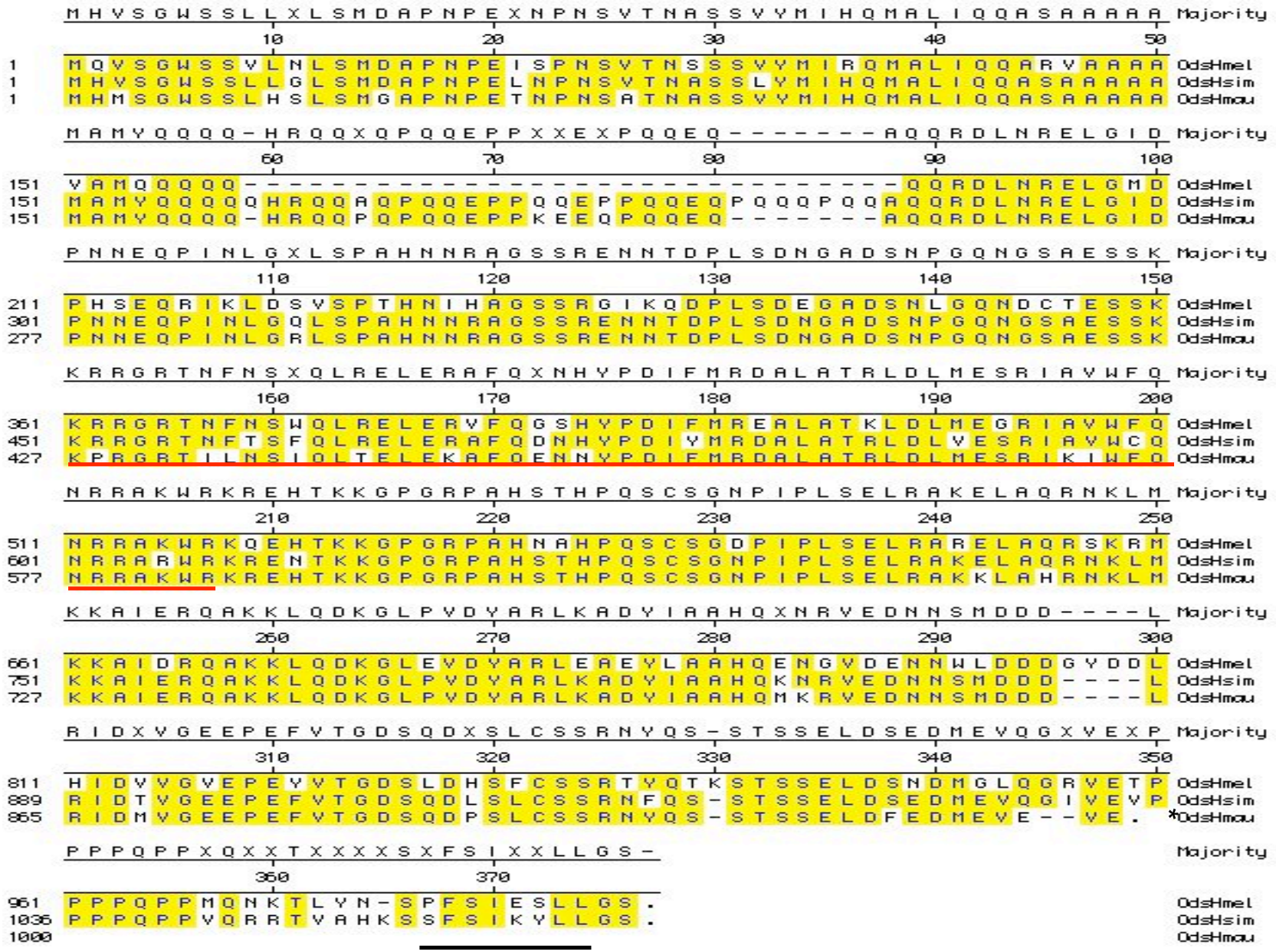

Fig. 15.—The alignment of three *OdsH* alleles. The homeodomain is labeled by the red under line, and the eh1 domain is labeled by the black under line.

In the *nanos>OdsH*^{mel} lines, only females have fertility defect but not males. The embryos produced from the females with the *OdsH*^{mel} expression have developmental defect. In these embryos, the nuclei cannot divide to individual nucleolus in the syncytial blastoderm and overlap to each other. It suggested that the expression of the *OdsH*^{mel} may influence the cell cycle procedure. While the expression of *OdsH* alleles from *D. simulans* seems has no defect in the males and females fertility. In addition, the morphology of the reproductive organs are similar to the ones from w^{1118} in both males and females. It may due to the lower expression level that can be seen in the RT-PCR, and may be there are subtle fertility effect in *nanos>OdsH*^{sim}.

According to the germlines analysis, *OdsH*^{mel} may play a role in cell cycle regulation. To confirm this hypothesis, *Drosophila* eye development provides a good model system.

OdsH expression in _Drosophila_ eye

The defect of the eye phenotype between heterozygous and homozygous strains with *OdsH*^{mel} expression showed the correlation with the mutant eye phenotype and the dosage of the *OdsH* allele. Only one copy of *OdsH* is sufficient to interference eye development and reduced adult eye size. As in Fig. 10. *GMR>OdsH*^{sim} and *GMR>OdsH*^{mau} flies also have small eye phenotype and lose normal ommatidia structure. The degree of the eye defect, by measuring the width of the eyes from three ectopic expression lines, is correlated to the sequence divergence. The nonsynonymous (Ka) and synonymous (Ks) ratio in *OdsH* of the five species in *Drosophila* shows that the ratio is 0.649 between *D. melanogaster* and *D. simulans*, 0.812 between *D. melanogaster* and *D. mauritiana*, and the highest ratio is between *D.*

mauritiana and *D. simulans*, in a value of 2.542 (Ting et al. 2004). *OdsH* from *D. melanogaster* have the strongest effect in eye development than *D. simulans* and the minor one from *D. mauritiana.* This result is consistent to previous observation in male fertility test. Under *D. melanogaster* background, $OdsH^{sim}$ and $OdsH^{mau}$ alleles also can increase male fertility like $OdsH^{mel}$ do, but the average influences are $OdsH^{mel} > OdsH^{sim} > OdsH^{mau}$ (Chen 2005). Combine these analysis, the divergence of the sequence might influence the intensity of *OdsH* to implement its function.

OdsH influence the M phase of the cell cycle

The adult eyes of *Drosophila* are developed from monolayer epithelia, called eye imaginal discs. Beginning with third-instars larva, a wave of cells called morphogenetic furrow (MF) sweeps across the eye disc from the posterior to the anterior. Cell posterior to the furrow divide and differentiate to form the ommatidial preclusters. The narrow band posterior to the MF arrest in G2, named second mitotic wave (SMW). In this wave, the cycling cells will enter the synchronized cell division process when receive the signal from ommatidia (Ready et al. 1976; Carthew 2007; Wolff 1991). According to the immunostaining, the mitotic cell numbers at the second mitotic wave were increased, when expressed $OdsH^{mel}$ in the third-instar larva, compared to the index of w^{1118}. Since the eye development of *Drosophila* is tightly regulated between cell division and differentiation. Genes that interfere with cell-cycle regulation will interrupt cell differentiation and resulting in different adult eye phenotypes.

In the normal eye development, it takes about 15 mins for cells at the SMW undergo syncitial cell mitotic. If $GMR>OdsH^{mel}$ inducing more cells to replicate, the mitotic cell index will increase. However, this is not the case in the *OdsH* expression.

The S phase cell numbers were similar in the eye discs no matter the *OdsH*^{mel} express or not. Thus, the increase of the mitotic cell was caused by the mitotic defect. Therefore, the molecular mechanism for the function of the *OdsH*^{mel} is playing a role in cell cycle regulation and focus on the M phase.

There is an example that overexpression the endogenous homeodomain contain gene in the *Drosophila* eye caused mitotic defect. *Pax6* is the members of a set of the transcription factors network that coexpress in the retinal precursor cells before cell differentiation to control the eye development. This gene contains two DNA-binding domain including the homeodomain and a transactivation domain. The splice variants of *Pax6,* Pax6p46 was observed to bind chromosome in the precentromeric region and resulted in abnormal eye development because of the mitosis defect (Zaccarini et al. 2007).

Recent data in the *D. simulans* cell culture system showed that the *OdsH* of *D. mauritiana* and *D. simulans* co-localized to the pericentric satellite DNAs, and *OdsH* of *D. mauritiana* bind to an extra locus (Bayes 2008). Combine the mitotic defect in the third-instar larva showed in ectopic expression flies, it is possible that *OdsH* participates in cell division by direct interaction with the chromosome. This might be the hint for us to think about the hybrid male sterility from the cross between *D. simluans* and *D. mauritiana*. The spermatogenesis process in *Drosophila* begins with primordial germ cells. Following one time of cell mitotic, primary spermatocyte was produced from the spermatogonia, which developed from the germ cells. Primary spermatocyte will then undergo two times of meiosis to generate four spermatids and will finally develop into four sperms (Fuller 1998; Gönczy and DiNardo 1996; Lin et al. 1994). In the spermatogenesis of the F1 hybrid males between *D. simluans* and *D. mauritiana*, some onion cells show a disparity in size between the nucleus and the

mitochondrial (Perez at al. 1993). With the understanding of the molecular mechanism and these information about *OdsH*, I proposed that the hybrid males sterility is caused by the problems in the division procedures in spermatogenesis. Furthermore, this mechanism for speciation would support the "centromere-drive" model (Malik and Henikoff 2002).

Henikoff and Malik brought up an idea that centromeric DNA sequences might play a special role in Haldane's rule (Malik and Henikoff 2001; Malik et al. 2002). They suggested that the rapid evolution of centromeric DNA reflects an arms race. During female meiosis, homologous chromosomes compete with each other to be the only one of four meiotic products that arrives in an egg in most species. Although centromere drive is a well known mechanism in mammals (de Villena and Sapienza 2001; Henikoff et al. 2001), it brings the cost— heterochromatic differences between paired chromosomes in *Drosophila* males at meiosis I would cause non-disjunction and result in unequal sex ratio or sterility (Fig. 16).

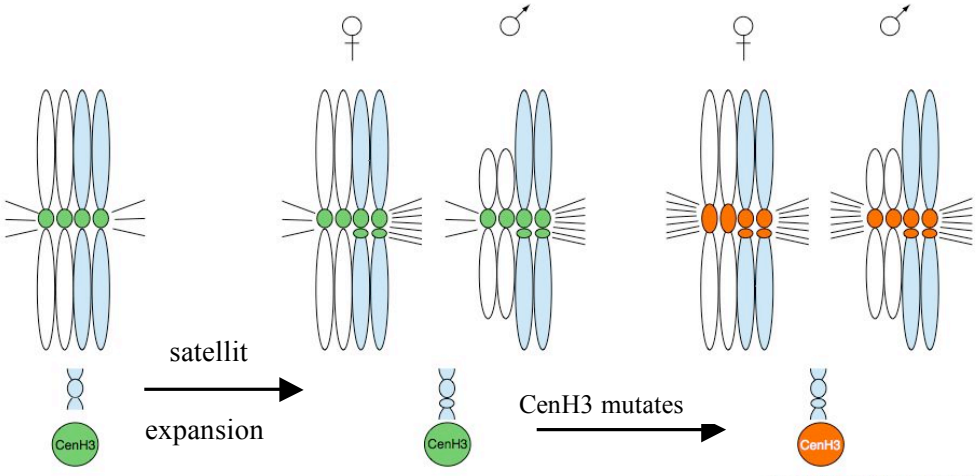

Fig. 16.—The centromere-drive model. There are two steps in this model. First, expansion in the satellite sequence of the centromere lead to more microtubule binding sites, which can result in a transmission advantage in female meiosis. This would cause deleterious effects in males, such as non-disjunction between the X–Y chromosomes. Second, a suppressor allele in centromeric histone H3 (CenH3) that can recover the equality of meiotic will be selectively favored. By expanding CenH3 binding and increasing microtubule attachments on the Y centromere the deleterious effects of centromere-drive will be lightened. (Malik et al. 2002)

According to studies here, the molecular mechanism of *OdsH*^{mel} was suggested to play a role in cell division. Whether hybrid male sterility between *D. mauritiana* and *D. simulans* is resulted from the cell division defect in the spermatogenesis process is now interested in further analysis. In addition, it is also important to understand the function of the amino acids substitution and the Eh1 domain in *OdsH*^{mel}.

Reference

Bateman JR, Lee AM, Wu CT. 2006. Site-specific transformation of *Drosophila via* ϕC31 integrase-mediated cassette exchange. Genetics. 173:769-777.

Baker NE. 2001. Cell proliferation, survival, and death in the *Drosophila* eye. Semin Cell Dev Biol. 12:499-507. Review.

Bayes JJ, Findlay GD, Malik HS. 2008. Cytological characterization of a hybrid sterility gene in *Drosophila*.

Bischof J, Maeda RK, Hediger M, Karch F, Basler K. 2007. An optimized transgenesis system for *Drosophila* using germ-line-specific ϕC31 integrases. Proc Natl Acad Sci U S A. 104:3312-3317

Brand AH, Perrimon N. 1993. Targeted gene expression as a means of altering cell fates and generating dominant phenotypes. Development. 118:401-415.

Brennecke J, Hipfner DR, Stark A, Russell RB, Cohen SM. 2003. *bantam* encodes a developmentally regulated microRNA that controls cell proliferation and regulates the proapoptotic gene hid in *Drosophila*. Cell. 113:25-36.

Brideau NJ, Flores HA, Wang J, Maheshwari S, Wang X, Barbash DA. 2006. Two Dobzhansky-Muller genes interact to cause hybrid lethality in *Drosophila*. Science. 314:1292-1295.

Buscarlet M, Stifani S. 2007. The 'Marx' of Groucho on development and disease. Trends Cell Biol. 17:353-361.

Carrington JC, Ambros V. 2003. Role of microRNAs in plant and animal development. Science. 301:336-338. Review.

Carthew RW. 2007. Pattern formation in the *Drosophila* eye. Curr Opin Genet Dev. 17:309-313.

Chen CH, Huang H, Ward CM, Su JT, Schaeffer LV, Guo M, Hay BA. 2007. A synthetic maternal-effect selfish genetic element drives population replacement in *Drosophila*. Science. 316:597-600.

Chen YL. 2005. Functional diversity of *Odysseus* (*OdsH*) and its role in spermatogenesis. Master thesis, National Tsing Hua University, Taiwan.

Clarkson M, Saint R. 1999. A *His2AvDGFP* fusion gene complements a lethal *His2AvD* mutant allele and provides an *in vivo* marker for *Drosophila* chromosome behavior. DNA Cell Biol. 18:457-462.

Coyne JA. 1985. The genetic basis of Haldane's rule. Nature. 314:736-738.

Coyne JA, Charlesworth B. 1986. Location of an X-linked factor causing sterility in male hybrids of *Drosophila simulans* and *D. mauritiana*. Heredity. 57:243-246.

Coyne T, Orr H. 2004 *Speciation*. Sinauer Associates, Sunderland, MA.

Darwin C. 1895 *On the Origin of Species by Means of Natural Selection*. Murray, London.

Denli AM, Tops BB, Plasterk RH, Ketting RF, Hannon GJ. 2004. Processing of primary microRNAs by the Microprocessor complex. Nature. 432:231-235.

Domínguez M, Wasserman JD, Freeman M. 1998. Multiple functions of the EGF receptor in *Drosophila* eye development. Curr Biol. 8:1039 -1048.

Duffy JB. 2002. GAL4 system in Drosophila: a fly geneticist's Swiss army knife. Genesis. 34:1-15.

Fish MP, Groth AC, Calos MP, Nusse R. 2007. Creating transgenic *Drosophila* by microinjecting the site-specific ϕC31 integrase mRNA and a transgene-containing donor plasmid. Nat Protoc. 10:2325-2531.

Freeman M. 1996. Reiterative use of the EGF receptor triggers differentiation of all cell types in the Drosophila eye. Cell. 87:651-660.

Fuller MT. 1998. Genetic control of cell proliferation and differentiation in *Drosophila* spermatogenesis. Semin Cell Dev Biol. 4:433-444.

Gönczy P, DiNardo S. 1996. The germ line regulates somatic cyst cell proliferation and fate during *Drosophila* spermatogenesis. Development. 122:2437-2447.

Grossniklaus U, Bellen HJ, Wilson C, Gehring WJ. 1989. P-element-mediated enhancer detection applied to the study of oogenesis in *Drosophila*. Development. 107:189-200.

Groth AC, Fish M, Nusse R, Calos MP. 2004. Construction of transgenic *Drosophila* by using the site-specific integrase from phage øC31. Genetics. 166:1775-1782.

Henikoff S, Ahmad K, Malik HS. 2001. The centromere paradox: stable inheritance with rapidly evolving DNA. Science. 293:1098-1102. Review.

Lagos-Quintana M, Rauhut R, Yalcin A, Meyer J, Lendeckel W, Tuschl T. 2002. Identification of tissue-specific microRNAs from mouse. Curr Biol. 12:735-739.

Lau NC, Lim LP, Weinstein EG, Bartel DP. 2001. An abundant class of tiny RNAs with probable regulatory roles in *Caenorhabditis elegans*. Science. 294:858-882.

Lee T, Luo L. 1999. Mosaic analysis with a repressible cell marker for studies of gene function in neuronal morphogenesis. Neuron. 22:451-461.

Levis R, Hazelrigg T, Rubin GM. 1985. Separable cis-acting control elements for expression of the white gene of *Drosophila*. EMBO J. 4:3489-3499.

Llave C, Kasschau KD, Rector MA, Carrington JC. 2002. Endogenous and silencing-associated small RNAs in plants. Plant Cell. 14:1605-1619.

Lin DM, Goodman CS. 1994. Ectopic and increased expression of Fasciclin II alters motoneuron growth cone guidance. Neuron. 13: 507-523.

Lin H, Yue L, Spradling AC. 1994. The Drosophila fusome, a germline-specific organelle, contains membrane skeletal proteins and functions in cyst formation. Development. 120:947-56.

Liu J, Carmell MA, Rivas FV, Marsden CG, Thomson JM, Song JJ, Hammond SM, Joshua-Tor L, Hannon GJ. 2004 Argonaute2 is the catalytic engine of mammalian RNAi. Science. 305:1437-1441.

Malik HS, Henikoff S. 2001. Adaptive evolution of Cid, a centromere-specific histone in *Drosophila*. Genetics. 157:1293-1298.

Malik HS, Vermaak D, Henikoff S. 2002. Recurrent evolution of DNA-binding motifs in the *Drosophila* centromeric histone. Proc Natl Acad Sci U S A. 99:1449-1454.

Malik HS, Henikoff S. 2002. Conflict begets complexity: the evolution of centromeres. Curr Opin Genet Dev. 12:711-718.

Masly JP, Jones CD, Noor MA, Locke J, Orr HA. 2006. Gene transposition as a cause of hybrid sterility in *Drosophila*. Science. 313:1448-1450.

Mayr E. 1963 *Animal Species and Evolution*. Belknap Press, Combridge, MA.

Pai CY, Kuo TS, Jaw TJ, Kurant E, Chen CT, Bessarab DA, Salzberg A, Sun YH. 1998. The Homothorax homeoprotein activates the nuclear localization of another homeoprotein, extradenticle, and suppresses eye development in Drosophila. Genes Dev. 12:435-446.

Pardo-Manuel de Villena F, Sapienza C. 2001. Female meiosis drives karyotypic evolution in mammals. Genetics. 159:1179-1189.

Presgraves DC, Balagopalan L, Abmayr SM, Orr HA. 2003. Adaptive evolution drives divergence of a hybrid inviability gene between two species of *Drosophila*. Nature. 423:715-719.

Perez DE, Wu CI, Johnson NA, Wu ML. 1993. Genetics of reproductive isolation in the *Drosophila simulans* clade: DNA marker-assisted mapping and characterization of a hybrid-male sterility gene, *Odysseus* (*Ods*). Genetics. 134:261-275.

Ready DF, Hanson TE, Benzer S. 1976. Development of the *Drosophila* retina, a neurocrystalline lattice. Dev Biol. 53:217-240.

Riz I, Lee HJ, Baxter KK, Behnam R, Hawley TS, Hawley RG. 2009. Transcriptional activation by TLX1/HOX11 involves Gro/TLE corepressors. Biochem Biophys Res Commun. 380:361-365.

Rørth P. 1998. Gal4 in the *Drosophila* female germline. Mech Dev. 78:113-118.

Saito K, Ishizuka A, Siomi H, Siomi MC. 2005. Processing of pre-microRNAs by the Dicer-1-Loquacious complex in *Drosophila* cells. PLoS Biol. 7:1202-1212.

Secombe J, Pispa J, Saint R, Richardson H. 1998. Analysis of a *Drosophila* cyclin E hypomorphic mutation suggests a novel role for cyclin E in cell proliferation. Genetics. 149:1867–1882.

Serano TL, Cheung HK, Frank LH, Cohen RS. 1994. P element transformation vectors for studying *Drosophila melanogaster* oogenesis and early embryogenesis. Gene. 138:181-186.

Spradling AC. 1993. Developmental genetics of oogenesis. Cold Spring Harbor Press, Cold Spring Harbor, NY. 1-70

Sun S, Ting CT, Wu CI. 2004 The normal function of a speciation gene, *Odysseus*, and its hybrid sterility effect. Science. 305:81-83.

Tabuchi K, Yoshikawa S, Yuasa Y, Sawamoto K, Okano H. 1998. A novel *Drosophila* paired-like homeobox gene related to *Caenorhabditis elegans unc-4* is expressed in subsets of postmitotic neurons and epidermal cells. Neurosci Lett. 257:49-52.

Tang S, Presgraves DC. 2009. Evolution of the *Drosophila* nuclear pore complex results in multiple hybrid incompatibilities. Science. 323:779-782.

Theurkauf WE. 1992. Behavior of structurally divergent alpha-tubulin isotypes during Drosophila embryogenesis: evidence for post-translational regulation of isotype abundance. Dev Biol. 154:205-217.

Ting CT, Tsaur SC, Wu ML, Wu CI. 1998. A rapidly evolving homeobox at the site of a hybrid sterility gene. Science. 282:1501-1504.

Ting CT, Tsaur SC, Sun S, Browne WE, Chen YC, Patel NH, Wu CI. 2004. Gene duplication and speciation in *Drosophila*: evidence from the *Odysseus* locus. Proc Natl Acad Sci U S A. 101:12232-12235

Van Doren M, Williamson AL, Lehmann R. 1998. Regulation of zygotic gene expression in Drosophila primordial germ cells. Curr Biol. 8:243-246.

White-Cooper H, Schafer MA, Alphey LS, Fuller MT. 1998. Transcriptional and post-transcriptional control mechanisms coordinate the onset of spermatid differentiation with meiosis I in *Drosophila*. Development. 125:125–134.

Winnier AR, Meir JY, Ross JM, Tavernarakis N, Driscoll M, Ishihara T, Katsura I, Miller DM 3rd. 2007. UNC-4/UNC-37-dependent repression of motor neuron-specific genes controls synaptic choice in *Caenorhabditis elegans*. Genes Dev. 13:2774-2786.

Wolff T, Ready DF. 1991. Cell death in normal and rough eye mutants of *Drosophila*. Development. 113:825-839.

Wolff T, Ready DF. 1991. The beginning of pattern formation in the *Drosophila* compound eye: the morphogenetic furrow and the second mitotic wave. Development. 113:841-850.

Yang CP, Chen MS, Liaw GJ, Chen SF, Chou G, Fan SS. 2005. Using *Drosophila* eye as a model system to characterize the function of mars gene in cell-cycle regulation. Exp Cell Res. 307:183-193.

Zaccarini R, Cordelières FP, Martin P, Saule S. 2007. Pax6p46 binds chromosomes in the pericentromeric region and induces a mitosis defect when overexpressed. Invest Ophthalmol. Vis Sci. 48:5408-5419.

Appendix

1. Generate the germline available site specific transgenic vector

The original transgenic vector *pUAST* has been proven to be useful for generating transgenic lines with UAS-target gene constructs in *Drosophila*. Such transgenic lines allow for conditional gene expression. In addition to the Gal4 binding sites that responds to the Gal4 activator, the vector *pUAST* contains a basal promoter from the hsp70 gene, a multiple cloning sites and the 3' region of SV40 (Fig. 17). However, heat shock induced expression using the full hsp70 promoter is inefficient in the germline (Brand and Perrimon 1993). This could be because the activity of the hsp70 promoter is reduced in germline cells. Therefore, an improved system for germline transformation called *pUASP* was devised. In this vector, the P transposase minimal promoter was chosen to replace the hsp70 promoter. Upstream the promoter are 14 Gal4 binding sites and GAGA sites from the EP vector. The P transposase minimal promoter has been shown to drive efficient expression in the germline during oogenesis (Grossniklaus et al. 1989). In addition, the sequences from the K10 gene, which promote the early transfer of RNAs from nurse cells into the oocyte, was added to further increase the efficiency of transfection. RNAs that contain the K10 sequence are transferred into the oocyte during the early to middle stages of oogenesis (i.e., during stages 2-9), while RNAs that lack this sequences are stored in nurse cells until stage 11. After these modifications, the resulting vector is named *pUASP* (Fig. 18) (Serrano et al. 1994).

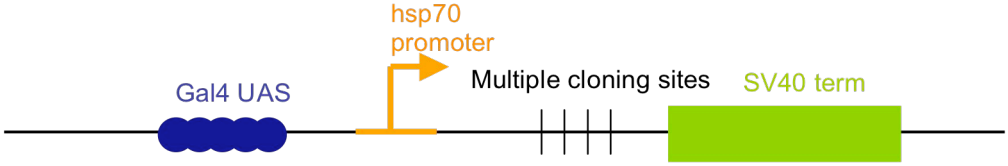

Fig. 17.—The *pUAST* transgenic vectors. In the original transgenic vector *pUAST*, there are five Gal4 binding sites upstream of the hsp70 promoter. Downstream of the promoter are the multiple cloning sites and the SV40 in the 3' region. (Rørth 1998)

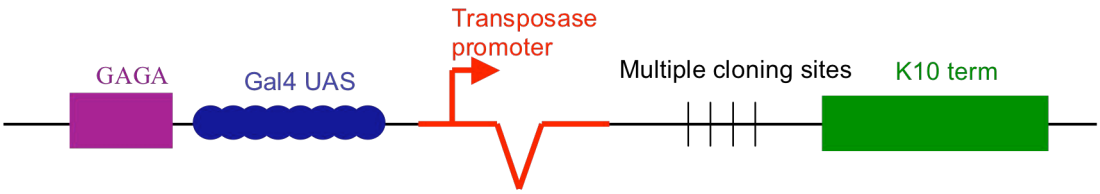

Fig. 18.—The *pUASP* transgenic vectors. In the *pUASP*, there are 2 GAGA sites and 14X Gal4 binding sites in the upstream of the P transposase minimal promoter. Next to the promoter region are the multiple cloning sites and then the 3'-UTR sequence and terminator from the K10 gene. The 3'-UTR sequence is used for stabilizing the transcripts in the germline cells without affecting the localization. (Rørth 1998)

Since the P element insertion occurs randomly, position effect can be problematic as gene expression can be vary strongly depending on the location of insertion. Therefore, phenotypic analysis would be difficult (Levis et al. 1985). The *ϕC31*-mediated integration is now an important mechanism to generate stie specific insertion lines. The unidirectional site-specific recombination is mediated by *Streptomyces* phage *ϕC31,* which encodes a serine integrase that carries out the sequence-directed integration between the phage attachment site attP in the phage genome and the bacterial attachment site attB in the host bacterial chromosome. In the *Drosophila* genome, several endogenous pseudo *attP* sites were identified and are recognized by the integrase (Fig. 19). This system has been established in the *Drosophila* by adding the attB sequence into the original transgenic vector *pUAST* and come out the site specific transgenic vector called *pUAST attB* (Groth et al. 2004). Furthermore, a collection lines with precisely mapped *attP* sites, and the endogenous sources of the *ϕC31* integrase also has been established (Bischof et al. 2007). In this study, I modified the *pUAST attB* site specific transgenic vector that is suitable for female germline expression first.

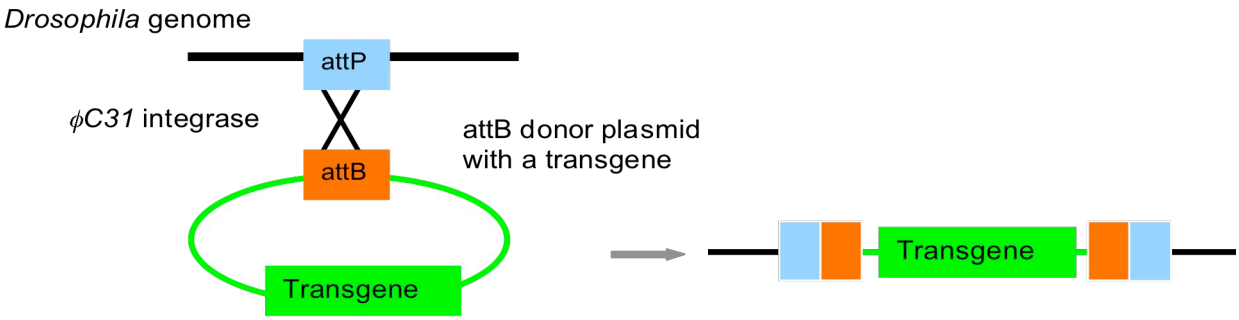

Fig. 19.— Site-specific integration mediated by *ϕC31*. The schematic outlining *ϕC31*-mediated integration. The fly endogenous integrase will recognize the attP sequence on the genome and mediated the recombination event between attB and attP, the transgene will then insert to the fly genome. (Fish et al. 2007)

In order to get the modified site specific integration vector that suitable for the germ line cells expression. The transgenic vector would contain 2 GAGA sites, 14X Gal4 binding sites, multiple cloning site and the K10 polyA signal sequence, which can be obtained from the P-element transposon vector UASp (*pUASP)* transgenic vector, and the attB sequence, loxP and white gene, which can be acquired from the *pUAST attB* transgenic vector. This can be done by restriction enzyme digestion of the two vectors followed by ligation of the desired fragments. The treatment of two vectors are shown below:

pUASP

First, double digestion of *pUASP*, 9939bp in size, with restriction enzymes *EcoR*V and *Pst*I was carried out. The *EcoR*V cutting site is at 9859bp, and would result in blunt ends. The *Pst*I cutting site is at 2220bp and would result in sticky ends. The product of these treatments is a segment of 2300bp in length spanning the regions important for the transgenic vector as described above. Second, the digested fragment was isolated with gel extraction. Lastly, to blunt the *Pst*I cutting site, the fragment was treated with the Klenow enzyme, which is the large fragment of DNA

polymerase I. After these steps, the fragment will be the insert in the subsequent ligation reaction.

pUAST attB

The *pUAST attB* contains attB sequence, SV40, 5XUAS-hsp70, loxP, white gene, T7, and T3 primers (Fig. 20). In order to replace the segment with 5XUAS-hsp70, multiple cloning sites, and SV40 signal sequence in the *pUAST attB*. *pUAST attB* transgenic vector was treated with the restriction enzyme *BamH*I. There are two cutting sites for *BamH*I in the vector: one at 4849bp and the other at 5980bp. The desired fragment is 7458bp in length. After performing the restriction enzyme digestion, by gel extraction the 7458bp band was isolated. The sticky ends of two *BamH*I sites were then blunted with the Klenow enzyme, and further treated with shrimp alkaline phosphatase (SAP) for dephosphorylation. The resulting fragment is the vector in the subsequent ligation reaction.

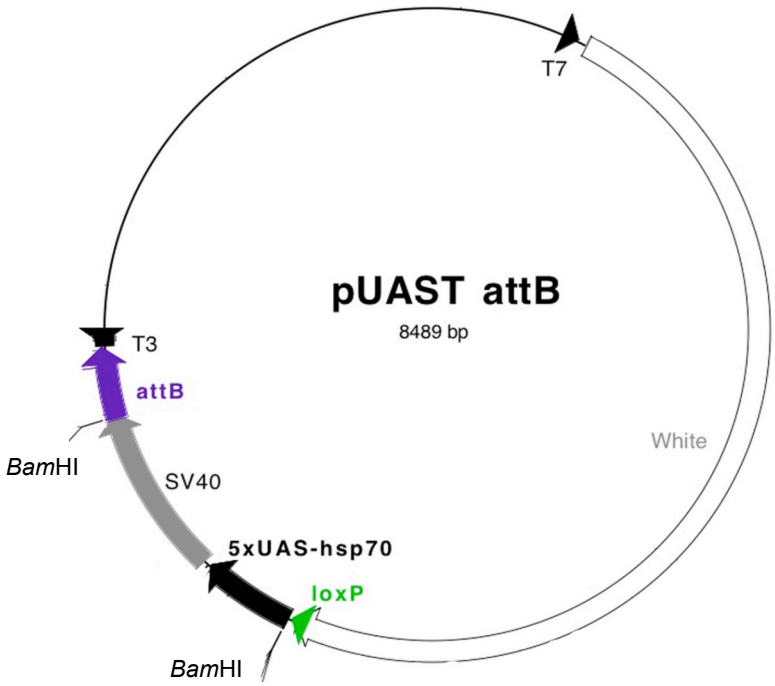

Fig. 20.—The site specific transgenic vector *pUAST attB*. The *pUAST attB* vector contains the white gene and the *attB* sequence. The attB site will recombine with attP to give site specific integration. SV40 here is different from the one used in the vector *pUAST*, with a 150bp deletion. Dash means the restriction enzyme site for *Bam*HI.

Ligation

For ligation, the insert is from *pUASP* and the vector is from *pUAST attB*. The two fragments were incubated with T4 ligase at 16ºC overnight. The product was then used to transform XL1-Blue competent cells, which were then grown overnight at 37ºC on LB plates with ampicillin. After checking the size of the plasmids, five colonies were picked as candidates containing the modified transgenic vector. These five candidates were larger in size than the *pUAST attB*. These five plasmids were also linearized by single restriction enzyme digestion with *Xba*I; all were similar in size.

To confirm whether these are actually the vectors intended, they were first sequenced with T3 primer. Sequencing results showed that only one plasmid had the correct insert sequence and the correct orientation. However, since sequencing is limited to about 600bp and the insert should be 2300bp, it was still unclear if the full-length insert is contained in the *pUAST attB*. Therefore, the plasmid with the correct sequence and the correct orientation was then digested by the restriction enzymes: *Nhe*I and *Spe*I. The intended vector I designed should have two *Spe*I sites and one *Nhe*I site, and thus digestion will yield five fragments of different sizes: 7010bp, 1503bp, 809bp, 291bp, and 40bp (Fig. 21). Notably, the presence of the 1503bp and 809bp bands signifies proper insertion and a complete insert. The restriction enzyme digestion confirmed that the vector is indeed the vector intended, and I named it *pUASP attB* (Fig. 22).

(A)

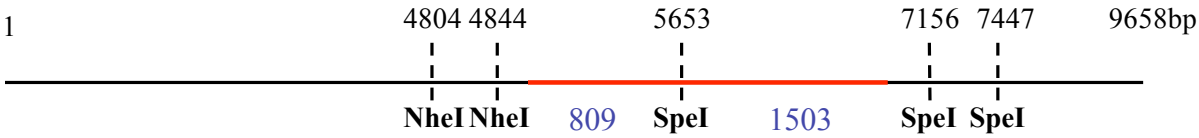

(B)

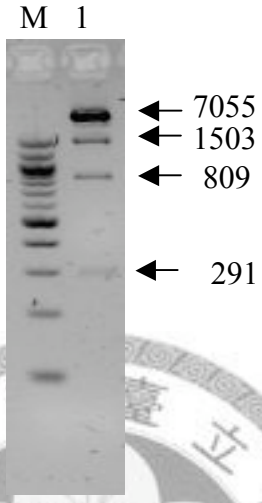

Fig. 21.—Restriction map of *pUASP attB* by *Nhe*I and *Spe*I. (A) The cutting sites of restriction enzymes *Nhe*I and *Spe*I were labeled. Numbers indicate the position in the vector and blue numbers indicate the length of the fragments after cutting. The red line signifies the insert. (B) The gel electrophesis picture show the digestion map of the candidate plasmid. The marker (lane M) was 100bp DNA ladder. Lane 1 is the result of the sample with the restriction enzyme digestion. Three bands from the bottom are 291bp, 849bp, and 1503bp. Large band that higher than marker is about 7055bp.

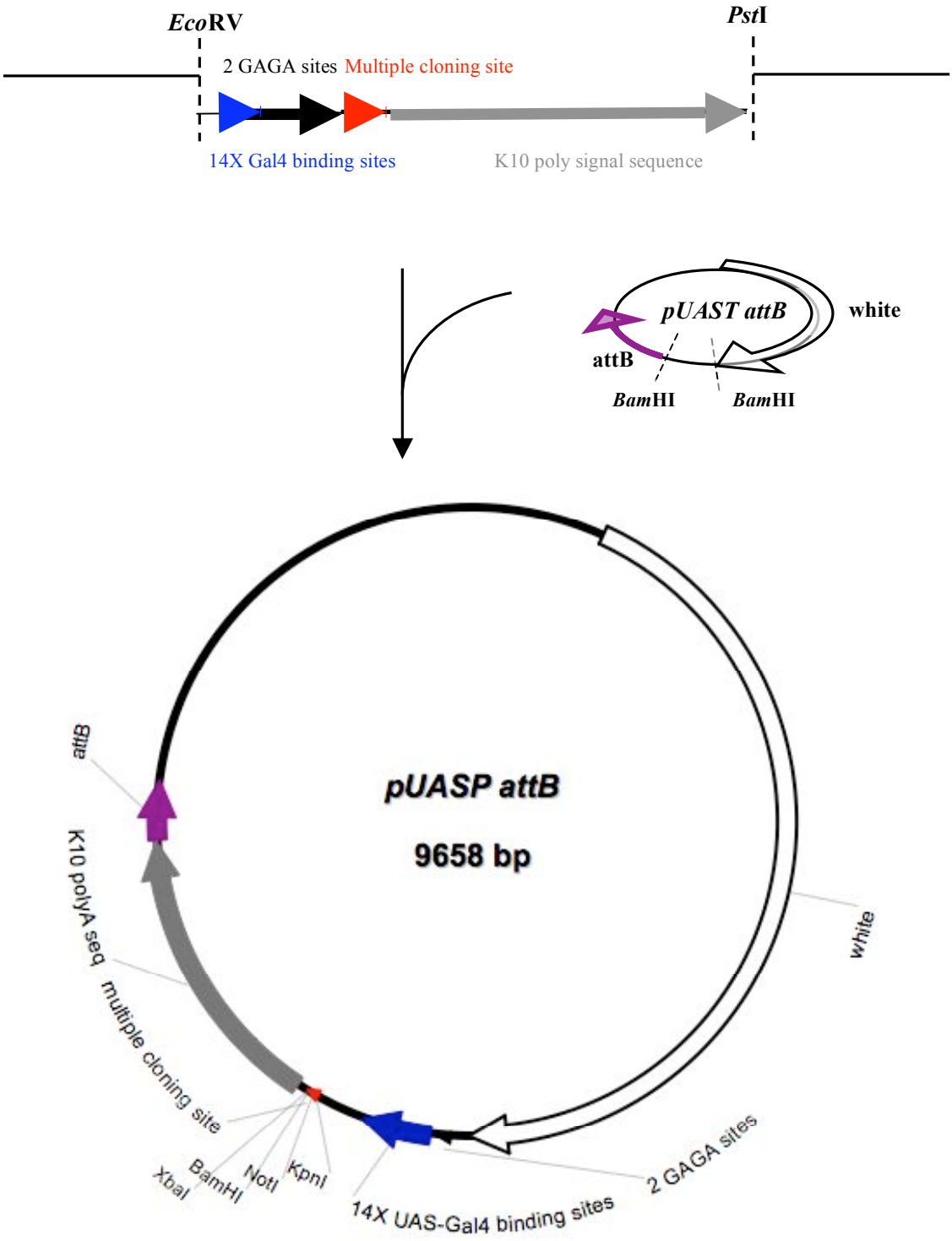

Fig. 22.—Procedure of the construct of *pUASP attB*. Dashes mean the digestion by the nearby restriction enzyme. The P-element transposon vector UASp (*pUASP*) was digested and subcloned into *pUAST attB* to get the final construct *pUASP attB* with total size 9658bp.

2. Generate the *unc-4* knockdown flies

Recently, hundreds of small RNAs of ~22 nucleotides, named microRNAs (miRNAs) have been discorved in animals and plants (Lau et al. 2001; Llave et al. 2002; Lagos-Quintana et al. 2002). The miRNAs have three different forms. First, it was transcribed as long primary transcripts (pri-miRNAs) and formed a hairpin loop structure. Following are two-step processing pathway: Drosha, which is the nuclease of the RNase III family, mediated the initial cleavage and the product called pre-miRNAs. After pre-miRNAs were exported to the cytoplasm, the further processed will act by Dicer and the mature miRNAs comes out. The mature miRNAs would cooperate with argonaute family proteins to carry out the gene silencing in complex form called "RISC". The predominant mechanism of silencing by "RISC" in animal is to interfere gene expression in the translation level (Denli et al. 2004; Saito et al. 2005; Liu et al. 2004).

miRNAs, interfere with the expression of the mRNA, which control the timing of the development, stem cell maintenance, and other developmental processed by binding to the complementary sequences on the target genes (Brennecke et al. 2003; Carrington et al. 2003). By the mechanism of miRNA-mediated silencing, the maternal-effect selfish genetic elements created in the *Drosophila* are resistant to the recombination-mediated dissociation of the drive and disease refractoriness functions (Chen et al. 2007). The efficiency of the designed RNA fragments, which apply the miRNA processing system in *Drosophila*, is high to knockdown the gene expression (Personal communication). According to the guides for the RNA fragment designed, his system was applied to generate the *unc-4* mutant.

A 22-nucleotide length target site in the 3'-UTR of the *unc-4* gene was selected. With the following 7 criteria: (1) a 22 nucleotides fragment, (2) contains 30-

52% GC, (3) at least 16-20% A or T, (4) the nucleotide number 20 must be A, (5) the 3rd nucleotide is better as A, (6) the nucleotide number 10 is better as T, and (7) the nucleotide number 13 should not be G. The criteria 3 and 4 are essential but 5 and 6 are optional.

The miRNA transcript should have four oligos to form a loop structure. The common two oligos for all with cloning sites are miR6_5'_*Not*I/*Bgl*II and miR6_3'_*Bam*HI/*Xba*I. The oligos that contain the sequence that target to the *unc-4* gene are miR6_*unc4*^{mel}_C for the target site sequence: CCAAAGCAATGCTTGAAATATG from 1646bp to 1669bp , and the miR6_*unc4*^{mel}_D for the target site sequence: AGAGTCCATTTCTCATGGAAAG from 2452bp to 2475bp. The designed oligo sequences are listed in Table 4.

Table 4
The sequences for the oligos for miR6_*unc4*^{mel}

Name	Sequence
miR6_5'_*Not*I/*Bgl*II	GGCGCGGCCGCCGCCAGATCTTTTAAAGTCCACAACTCATC AAGGAAAATGAAAGTCAAAGTTGGCAGCTTACTTAAACTTA
miR6_3'_*Bam*HI/*Xba*I	GGCCTCTAGAACGGATCCAAAACGGCATGGTTATTCGTGTG CCAAAAAAAAAAAAAATTAAATAATGATGTTAGGCAC
miR6_*unc4*^{mel}_C1	GGCAGCTTACTTAAACTTAATCACAGCCTTTAATGTCCAAA GCAATGCTTGAAATCTGTAAGTTAATATACCATATC
miR6_*unc4*^{mel}_C2	AATAATGATGTTAGGCACTTTAGGTACCCAAAGCAATGCT TGAAATATGTAGATATGGTATATTAACTTACAGA
miR6_*unc4*^{mel}_D1	GGCAGCTTACTTAAACTTAATCACAGCCTTTAATGTAGAGT CCATTTCTCATGGACAGTAAGTTAATATACCATATC
miR6_*unc4*^{mel}_D2	AATAATGATGTTAGGCACTTTAGGTACAGAGTCCATTTCTC ATGGAAAGTAGATATGGTATATTAACTTACTGT

The designed sequences of the oligos were used to predict the structure and the target site online (http://sfold.wadsworth.org/) (Fig. 23), and did the e cloning by the software sequence builder to check the designed oligos can match to the 3'-UTR

of the *unc-4* gene, and the oligos would form the loop structure. After these checking steps, did two rounds of PCR to generate the fragment that contained four oligos. Two fragments that target to two different sites of the 3'-UTR in the *unc-4,* were cloned into pCR2.1-TOPO® (Invitrogen) respectively. One of the TA clone were digested with the restriction enzymes *Bgl*II and *Hin*dIII to get the fragment as the insert in the next step. Another TA clone was digested with the restriction enzymes *Bam*HI and *Hin*dIII to get the fragment as the vector in the next step. After gel extraction, the insert and vector part from each digestion steps were ligated. The product from the ligation procedure was digested again with the restriction enzymes *Not*I and *Xba*I for preparing to clone into the transgenic vector *pUAST attB* and *pUASP attB*. The transgenic constructs were named *pP{5'-UAST::mir_unc4^{mel}}* and *pP{5'-UASP:: mir_unc4^{mel}}*.

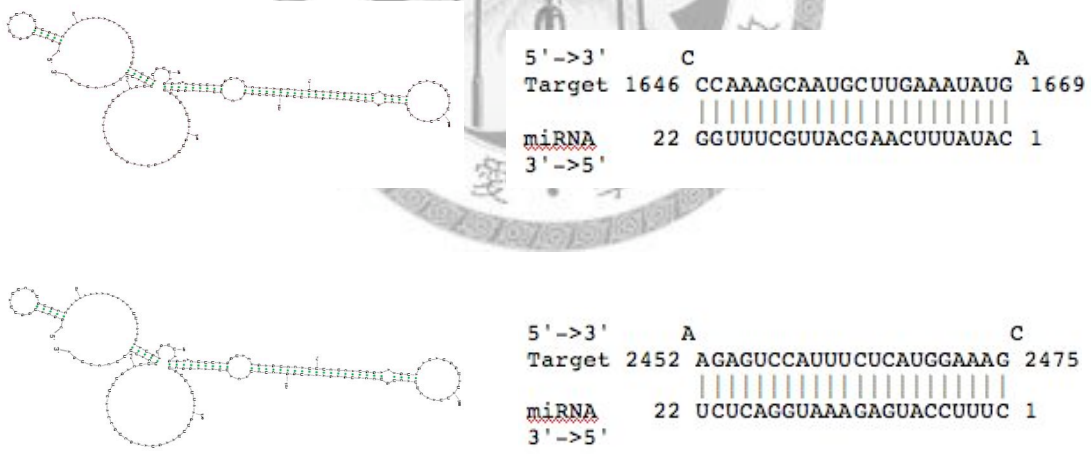

Fig. 23.—The target and structure prediction of two miRNA. There are two miRNA designed with the target sites in the 3'-UTR of *unc-4* gene. The upper one of the picture in this figure is named miR_*unc4^{mel}*_C, and the lower one is named miR_*unc4^{mel}*_D. In both two parts of the picture, the left ones are the predict structures, and the right ones are the predicted target sites.

The *mir_unc-4* transgenic lines

For the transgenic vector *pUAST attB*, *pP {5'-UAS::mir_unc-4^{mel}}* was injected into 34 embryos for each attP line, and 3 larvae of *ZH-attP-51D* line and 16 larvae of *ZH-attP-86Fa* line were collected. For another transgenic vector *pUASP attB*, 26 embryos were injected for each attP line, and 8 larvae of *ZH-attP-51D* line and 14 larvae of *ZH-attP-86Fa* line were collected. Only one transformant of each chromosome for each UAS constructs were obtained respectively (Table 5).

Table 5
The list of *UAS-mir_unc-4* transgenic lines

	Numbers of injected embryo	Numbers of hatched larvae	Transformant
pUAST attB vector			
ZH-attP-51D	34	3	1
ZH-attP-86Fa	34	16	1
pUASP attB vector			
ZH-attP-51D	26	8	1
ZH-attP-86Fa	26	14	1

The third chromosome insertion lines for each P-elenment construct were used to cross with different Gal4 lines, including *elav*-Gal4, *GMR*-Gal4, *nanos*-Gal4, and *tub*-Gal4, for functional analysis. All Gal4 lines chosen to drive *UAS-mir_unc-4* expression have no defect in the development of flies that all embryos in four lines can grow up to adult flies no matter what the transgenic vectors were used. The RT-PCR result showed that the expression of the *unc-4* gene in the *tub>mir_unc-4* are similar to the expression in w^{1118} (Fig. 24).

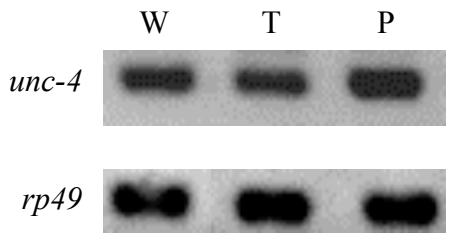

Fig. 24.—RT expression of *unc-4*. RNA were extracted from three different lines, including (w) w^{1118}, (T) *tub>mir_unc4*^{mel} (with the transgenic vector *pUAST attB*), and (P) *tub>mir_unc4*^{mel} (with the transgenic vector *pUASP attB*). All of them have the *unc-4* expression. *rp49* was used as the control gene in all samples.

According to the results of the phenotypic observation and the RT-PCR, the RNA interfere system seams invalidity. Several methods can be tried to improve this. First, design the miRNA that target to the sequence both in the coding region and the 3'-UTR region. Although the endogenous miRNA of the animals usually have the complementary sequence in the 3'-UTR of the gene that it regulated, the RNA fragments designed to apply the *Drosophila* endogenous miRNA system may have higher efficiency to deal with the coding region rather than the 3'-UTR. Second, raising the incubated temperature of the flies, when it crosses to Gal4 lines to induce the miRNA expression, because the activity of the Gal4 lines may increase with the higher temperature (Duffy 2002). Finally, increase the target sites of the gene, because the efficiency of the miRNA to knockdown the gene expression is not one hundred percent, more target sites may increase the probability to knockdown the gene.

Generate the *OdsH* knockdown flies

Except for the *unc-4* knockdown, *OdsH* knockdown flies were also desired to be generated. By following the miRNA designed criteria, the target site of *OdsH* is determined. The target site sequence: GATTTCGGGTGGTTAGCTAAGC is from the

1183bp to 1205bp in 3'-UTR of *OdsH*. The 3'-UTR sequence of *OdsH* is short thus only one suitable target site is chose. The common two oligos: miR6_5'_*Not*I/*Bgl*II and miR6_3'_*Bam*HI/*Xba*I were also used. The designed oligo sequences are listed in Table 6.

Table 6
The sequences for the oligos

Name	Sequence
miR6_5'_*Not*I/*Bgl*II	GGCGCGGCCGCCGCCAGATCTTTTAAAGTCCACAACTCATC AAGGAAAATGAAAGTCAAAGTTGGCAGCTTACTTAAACTTA
miR6_3'_*Bam*HI/*Xba*I	GGCCTCTAGAACGGATCCAAAACGGCATGGTTATTCGTGTG CCAAAAAAAAAAAAAATTAAATAATGATGTTAGGCAC
miR6_*OdsH*^{mel}_C1	GGCAGCTTACTTAAACTTAATCACAGCCTTTAATGTGATTTC GGGTGGTTAGCTACGCTAAGTTAATATACCATATC
miR6_*OdsH*^{mel}_C2	AATAATGATGTTAGGCACTTTAGGTACGATTTCGGGTGGTT AGCTAAGCTAGATATGGTATATTAACTTAGCGT

The transgenic constructs named *pP{5'-UASP::mir_OdsH*^{mel}*}* was generated following the procedures described in the *unc-4* part. To get the transgenic flies, *pP{5'-UASP::mir_OdsH*^{mel}*}* was injected into 38 embryos for each attP line, and 6 larvae of *ZH-attP-51D* line and 2 larvae of *ZH-attP-86Fa* line were collected. However, no transformant was obtained.

3. Solutions

10X Phosphate-buffered saline (10X PBS):

$NaH_2PO_4 \bullet H_2O$ ……..…….. 2.56g (18.6mM)
Na_2HPO_4 ……... 11.94g (84.1mM)
NaCl ……...…... 102.2g (1750mM)

Combine all components in <1 liter of ddH_2O and stir to dissolve. Adjust pH to 7.0 and final volume of 1 liter with ddH_2O. Sterilize by autoclaving.

1X Phosphate Buffered Saline Tween-20 (1X PBST):

0.3% Tween 20 in 1x PBS

4% Paraformaldehyde (fixation solution):

Paraformaldehyde …….. 4g
ddH_2O ……50ml
1N NaOH ……....1ml

Mixture gently and heat to 60-65 ºC until the paraformaldehyde is dissolved. Next add 10ml of 10X PBS and to cool to room temperature. Adjust pH to 7.4 and final volume of 100ml with ddH_2O. Finally, filter the solution through a 0.45-μm membrane filter.

3% BSA (blochking solution):

BSA …….. 3g
1X PBST ……..... 100ml

1,4-Diazabicyclo[2.2.2]octane (DABCO) (mounting solution):

N-propyl gallate ……..... 1.23g
10X PBS ……..... 5ml
100% glycerol ……45ml

4. Row Data

The width of the eye

	w^{1118}	*GMR>OdsH*^{mel}	*GMR>OdsH*^{sim}	*GMR>OdsH*^{mau}
1	338	175	170	261
2	340	205	188	220
3	323	158	186	182
4	396	173	260	233
5	321	164	215	250
6	313		219	235
7	313		215	258
Mean	334.86	175	207.57	234.14
SD	29.05	18.12	29.58	27.27

The mitotic index at the first and second mitotic wave

	w^{1118}		*GMR>OdsH*^{mel}	
	I	II	I	II
1	72	64	66	59
2	36	54	32	71
3	41	58	65	56
4	32	44	61	82
5	22	73	57	64
6	60	54	60	56
7	30	41	56	71
8	44	52	51	63
9	45	40	58	71
10	52	46	47	59
11	35	55	71	64
12	52	37	40	65
13	51	45	60	70
14	33	43	44	73
15	66	45	51	74
16	84	60	51	62
17	71	65	64	66
18	60	51	38	74
19	71	46	72	84
20			38	64
21			39	63
22			41	66
23			41	62
24			45	60
25			64	58
26			40	46
27			64	54
28			69	67
Mean	50.37	51.21	53.04	65.14
SD	17.23	9.62	11.76	8.24